UNIVERSITÄTSKLINIKUM HAMBURG-EPPENDORF

Klinik und Poliklinik für Gynäkologie

Direktorin: Prof. Dr. med. Barbara Schmalfeldt

Analysis on the Adhesive Properties of Ascites-derived Cells in Ovarian Cancer

Dissertation

zur Erlangung des Grades eines Doktors der Medizin
an der Medizinischen Fakultät der Universität Hamburg.

vorgelegt von

Yi Ding
aus Huaian

Hamburg 2019

(wird von der Medizinischen Fakultät ausgefüllt)

Angenommen von der
Medizinischen Fakultät der Universität Hamburg am: 21.07.2020

Veröffentlicht mit Genehmigung der
Medizinischen Fakultät der Universität Hamburg.

Prüfungsausschuss, der/die Vorsitzende: PD Dr. Leticia Oliveira-Ferrer

Prüfungsausschuss, zweite/r Gutachter/in: PD Dr. Christine Stürken

Figure Contents

Table contents

1 Introduction

1.1 Ovarian Cancer

Ovarian cancer (OvCa) is the most lethal gynecologic malignancy and the fifth cause of cancer death in women worldwide. Frequently asymptomatic at an early-stage leads to more than 70% of OvCa patients diagnosed at an advanced-stage with metastasis. Over one third of OvCa patients have malignant ascites formation at diagnosis, which is known to play a fundamental role in chemoresistence, metastasis and recurrence in the future [1]. Therefore, a thorough biological understanding of ascites and especially ascites-derived cells in the context of OvCa development and progression is urgently needed in order to establish more effective strategies for the treatment of OvCa.

1.1.1 Epidemiology and risk factors

Globally, 225,500 new cases of ovarian cancer are diagnosed each year, with 140,200 cancer-specific deaths. Incidence and survival rates vary by countries: Russia and the United Kingdom have the highest rates of ovarian cancer, whereas China has the lowest rates[2].

Several factors can increase the risk of developing ovarian cancer, including genetic factors, age, postmenopausal hormonal therapy use, infertility and nulliparity. In a range of genetic factors, germline BRCA1 and BRCA2 mutations are the most significant known genetic risk factors for OvCa and either mutations are found in up to 17% of patients[3, 4]. The use of oral contraceptives has been shown to reduce the risk of developing ovarian cancer in individuals with a germline BRCA1 mutation, as well as in those without a genetic predisposition[5, 6]. Retrospective factors, such as parity, prior tubal ligation, salpingectomy and unilateral or bilateral oophorectomy (surgical removal of the ovary) have been identified to influence the risk of ovarian cancer[7-9]. Additional risk factors, for instance, obesity is also a risk for poor outcomes following diagnosis of ovarian cancer [10], and meta-analyses have suggested a beneficial effect of regular physical activity on the risk of developing ovarian cancer, with a 30–60% reduction in risk in the most active women[11].

1.1.2 Histology and staging

Ovarian cancer has different histological subtypes. Epithelial cancers account for 90% of ovarian cancers and include serous, endometrioid, clear-cell and mucinous carcinomas. Of these types, high-grade serous carcinoma (HGSC) is the most commonly diagnosed. Non-epithelial ovarian cancers, including germ-cell tumors and sex cord stromal tumors, account for 10% of ovarian cancers[2].

Pathological evaluation and tumor staging of ovarian cancer is based on surgical assessment of the cancer at initial diagnosis, including removal of lymph nodes, tissue biopsy and abdominal fluid, and uses the International Federation of Gynecology and Obstetrics (FIGO) staging system[2].

Table 1 *Staging of ovarian cancer*

FIGO stage	Description	Corresponding TNM stage
I	Tumor confined to ovaries or fallopian tubes	T1
IA	Tumor limited to one ovary (with ovarian capsule intact) or fallopian tube; no tumor on ovarian or fallopian tube surface; no malignant cells in the ascites or peritoneal washings	T1a
IB	Tumor limited to both ovaries (with ovarian capsules intact) or fallopian tubes; no tumor on ovarian or fallopian tube surface; no malignant cells in the ascites or peritoneal washings	T1b
IC	Tumor limited to one or both ovaries or fallopian tubes, with any of the following C substages: • IC1: surgical spill intraoperatively • IC2: capsule ruptured before surgery or tumor on ovarian or fallopian tube surface • IC3: malignant cells in the ascites or peritoneal washings	T1c
II	Tumor involves one or both ovaries, or the fallopian tubes with pelvic extension below the pelvic brim or primary peritoneal cancer (Tp)	T2

IIA	Extension and/or implants of tumor on uterus and/or fallopian tubes and/or ovaries	T2a
IIB	Extension of tumor to other pelvic intraperitoneal tissues	T2b
III	Tumor involves one or both ovaries, or the fallopian tubes, or primary peritoneal cancer with cytologically or histologically confirmed spread to the peritoneum outside the pelvis and/or metastasis to the retroperitoneal lymph nodes	T3
IIIA	Metastasis to the retroperitoneal lymph nodes with or without microscopic peritoneal involvement beyond the pelvis	T1, T2, T3aN1
	IIIA1: positive retroperitoneal lymph nodes only (pathologically proven) • IIIA1(i): metastasis up to 10 mm in greatest dimension • IIIA1(ii): metastasis >10 mm in greatest dimension	T3a/T3aN1
	IIIA2: microscopic extrapelvic (above the pelvic brim) peritoneal involvement with or without positive retroperitoneal lymph nodes	T3a/T3aN1
IIIB	Macroscopic peritoneal metastasis beyond the pelvis up to 2 cm in greatest dimension, with or without metastasis to the retroperitoneal lymph nodes	T3b/T3bN1
IIIC	Macroscopic peritoneal metastasis beyond the pelvis >2 cm in greatest dimension, with or without metastasis to the retroperitoneal lymph nodes (includes extension of tumor to capsule of liver and spleen without parenchymal involvement of either organ)	T3c/T3cN1
IV	Distant metastasis excluding peritoneal metastases • IVA: pleural effusion with positive cytology • IVB: parenchymal metastases and metastases to extra-abdominal organs (including inguinal lymph nodes and lymph nodes outside of the abdominal cavity)	Any T, any N or M1

1.2 Ascites

Physiologically, ascites (peritoneal fluid) produced by capillary membranes can be reabsorbed into the lymphatic channels. However, in cases of disseminated intra-abdominal cancer, further increased production of ascites is induced by the tumors due to the increased permeability of tumor microvasculature and obstruction of the lymphatic vessels[12, 13]. The most common primary site of cancer that is associated with ascites is ovary, accounting for 38% of malignant ascites occurring in females[14]. The majority of women with ovarian cancer in advanced disease (stage III or stage IV) presents malignant ascites, which promotes the detached tumor cells to spread into other pelvic and peritoneal organs. Interestingly, in a study of 685 OvCa patients including 58% with ascites at the time of initial surgery, patients with an ascites volume greater than the median of 2000 mL had significantly shorter PFS (14.5 months vs. 22.7 months; $p < 0.001$) and OS (27.7 months vs. 42.9 months; $p < 0.001$)[15].

1.2.1 Cellular Components in the abdominal cavity

The origin and phenotype of cells in the ascites is not well understood. The cellular components include stroma cells and tumor cells. The stromal cells, also seen as non-malignant cell types, include fibroblasts, endothelial cells, mesothelial-like cells, adipocytes, and immune cells, which are associated with tumor cells[16, 17].

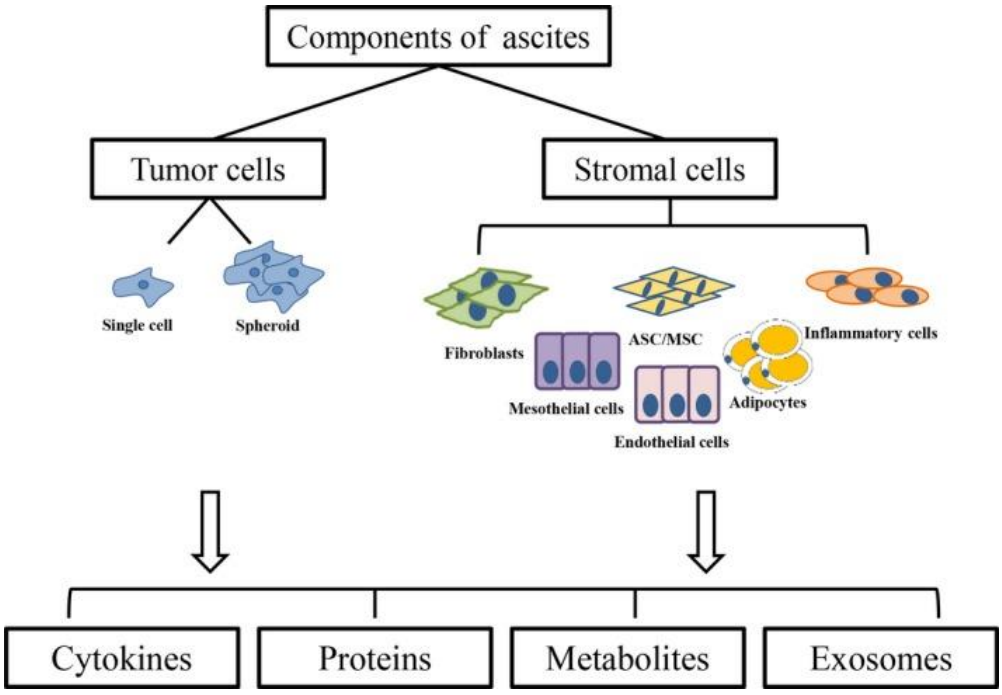

Figure 1 *Overview of cellular and acellular components of ascites*

Immune cells. Ascites contained different types of immune cells, including large numbers of different types of T cells[18], tumor-associated macrophages (TAMs)[19, 20], and other host cells, supporting tumor cell proliferation, progression, chemoresistance, and immune evasion[21-23]. Impairments of both innate immune cells and antitumor T cell response, cooperate with tumor cells to create a tumor-promoting and immunosuppressive tumor microenvironment (TME)[24]. The activity of immune effector cells, including CD4 T cells, CD8 T cells, and NK cells, is inhibited not only directly by tumor cells but also by immunesuppressive T regulatory cells (Tregs), immature dendritic cells (DCs), myeloid-derived suppressor cells (MDSCs), and tumor-associated macrophages (TAMs)[25-27].

TAMs, as a main innate immune cell population, have been described to play a crucial role in promoting tumor cell proliferation, dissemination, chemoresistance and immune evasion in different types of human cancer and mouse models, including ovarian high-grade serous cancer[28-30]. In OvCa, TAMs secrete multiple metastasis-promoting cytokines including IL-6, IL-10, CCL18, CCL22, TNFα, and TGFβ to support ovarian cancer cell adhesion and invasion[31, 32]. A recent study has revealed a surprising similarity between TAMs from ovarian cancer ascites and resident peritoneal macrophages with respect to their global transcriptional profile, the expression of differentiation markers, and their activation state[33]. TAMs from ovarian cancer ascites can indeed be shifted under experimental conditions to trigger a partial cytotoxic activity under experimental conditions[34, 35]. Consistent with these tumor-promoting functions of TAMs, expression of the alternative activation marker CD163 in TAMs from malignancy-associated ascites showed a strong correlation with early relapse of serous ovarian carcinoma after first-line therapy[36]. Recent data suggest that tumor-associated macrophages (TAMs) may promote spheroid formation and tumor growth in a mouse model[37].This group found that nearly 80% of macrophages infiltrated in the peritoneal cavity were detected in spheroids. Spheroid-associated TAMs were shown to secrete large amounts of epidermal growth factor (EGF), which leads to upregulation of integrin and ICAM-1 expression in tumor cells to form a positive autocrine feedback loop[37].

Additionally, it has been notified that increased accumulation of tumor-infiltrating lymphocytes (TILs) in OvCa patients delayed the recurrence of the disease and was

beneficial for survival[38]. The heightened infiltration of TILs was associated with increased level of the cytokines interferon (IFN)γ, which is a prognostic factor for longer survival and has been studied in clinical trials for treating ovarian carcinoma[39, 40]. Moreover, cytotoxic T cell infiltration in ovarian cancer has been shown to correlate with improvement in overall survival in several studies[41]. For example, antitumor immune responses composed of tumor-reactive T cells and tumor-specific antibodies can be detected in peripheral blood, ovarian cancer tissue and ascites[42-45]. Furthermore, cytotoxic T cell infiltration in ovarian tumors correlates with improvement in overall survival, as shown by several groups[45, 46].

Mesothelial-like cells. Mesothelial cells exfoliate from the peritoneal lining and float in the ascites[47]. Due to sustained inflammation, mesothelial cells lose epithelial-like properties, including dissolution of cell-cell junctions and their apical-basolateral polarity, and acquired a mesenchymal phenotype (mesothelial-to-mesenchymal transition (MMT) with increased migration and invasion capacities[47]. Mesothelial-derived cancer-associated fibroblasts (CAFs) share characteristics with myofibroblasts, such as the expression of alpha-smooth muscle actin (αSMA), fibroblast activation protein-α (FAPα) and fibroblast-specific protein 1 (FSP1)[48]. Exposure of myofibroblastic-like cells to ascites increased the secretion of VEGF and other pro-survival soluble factors[49, 50], further contributing to the evolution of the tumor environment[51].

Adipocytes. Mesenchymal stem cells (MSCs) may be easily derived and propagated from a variety of sources, including bone marrow and adipose tissue[52]. The omentum, the most common metastasis site for OvCa, is primarily composed of adipose tissue and milky spots [53]. Previous studies have demonstrated that adipose tissue contains an abundance of mesenchymal progenitor cells which promote tumor progression[54-56]. Adipose tissue-derived MSCs are favored in clinical trials of MSCs that secrete particular gene products into the cancer microenvironment[57, 58].

Tumor Cells. The ovarian surface epithelium, a single layer of cells covering the ovary, is derived from the coelomic epithelium, whereas the uterus, cervix, and fallopian tube develop from the müllerian (paramesonephric) ducts. Over the past 40 years, the idea that the single layer of ovarian surface epithelium (OSE) gives rise to serous carcinoma

gained wide acceptance[59, 60]. Recently, more evidence indicates that HGSCs can originate from epithelial cells lining the fallopian tube fimbriae, through a precursor lesion termed serous tubal intraepithelial carcinoma (STIC), which can be identified in 18–60% of cases of advanced-stage HGSCs and up to 80% of early-stage HGSCs[61-66].

During initial tumorigenesis, ovarian carcinoma cells undergo an epithelial-to-mesenchymal transition during invading into the peritoneum and retain mesenchymal properties, which involves a change in cadherin and integrin expression and upregulation of proteolytic pathways. Carried by the peritoneal fluid, ovarian tumor cells are either present as single cells or, more commonly, as aggregates of non-adherent cells, also known as spheroids[67]. The composition of spheroids are not well understand. However, a study group had found that spheroids contained one or more cores of myofibroblastic-like cells encased in a shell of tumor cells suggesting that free-floating tumor and stromal cells in the peritoneal effusions can interact with each other to form heterotypic spheroids(Figure2)[51]. Spheroids in the ascites present enhanced expression of E-cadherin, cell-to-cell contact and the ability of invasion, as well as reduced proliferation and limited drug penetration, especially those obtained from patients with chemoresistant recurrence[68].

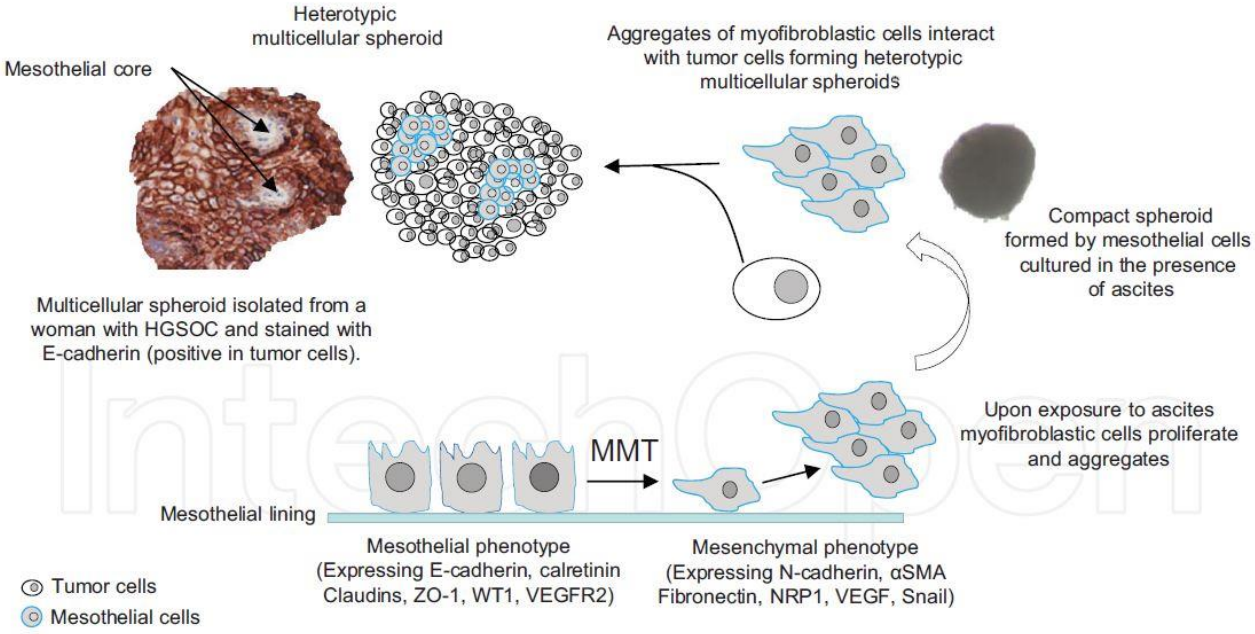

Figure 2 *Model for myofibroblast cells interactions with tumor cells and spheroids formation[51]*

1.2.2 Soluble Components

Malignant ascites consists of cytokines, chemokines, growth factors, and ECM fragments, which individually or in a combined way affect tumor cell growth and progression through different cellular mechanisms[69-72].

Cytokines. The concentration of proinflammatory cytokines such as IL- 6, IL-8, IL-10 was shown to be significantly higher in the ascites of ovarian cancer patients compared to that present in the serum, and correlated with poor prognosis and response to therapy[73, 74]. IL-6 not only promote tumor growth, migration, and invasion[73, 75, 76], but also facilitate chemoresistence in OvCa patients[77, 78]. The expression of IL-8 is associated with increased tumorigenicity and ascites formation in OvCa animal models[79, 80]. High levels of IL-6 and IL-10 expression in ascites have been shown to be associated with shorter progression-free survival[81], and poor initial response to chemotherapy[74].

Chemokines. Chemokines also have a role in the pathophysiology of ascites. CXCR4, the receptor for CXCL12, contributes to the proliferation[82] and migration[83] of EOC. The level of chemokine ligand CXCL4 is increased in ascites from patients with EOC[84].

Proteinases. MMPs, are crucial for invasive cancer growth and the pathogenesis of ascites. MMPs, mainly MMP9, have a role in the release of biologically active vascular endothelial growth factor (VEGF) and consequently in the formation of ascites[85] and have been shown to be an independent predictor of decreased survival in OvCa[86].

Growth Factors. Angiogenesis has a crucial role in the pathogenesis of epithelial ovarian cancer, promoting tumor growth and metastasis[87]. VEGF is one of the most potent proangiogenic factors identified in ovarian cancer, which is found at high levels in both the primary tumor, the ascites and the serum in ovarian cancer, and VEGF expression correlates with poor survival in ovarian cancer patients[88-90]. Other proangiogenic factors are also identified, including fibroblast growth factor, angiopoietins, endothelins, IL-6, IL-8, macrophage chemotactic proteins and platelet-derived growth factors[91, 92].

Other soluble components. LPA, a bioactive phospholipid, produced by ovarian cancer tumors, presents in high level in the ascites of ovarian cancer patients and plays an

important role in ovarian cancer metastasis[24]. The enzyme Transglutaminase, which is overexpressed in the ovarian cancer cells[93] and secreted into ascites[94], has been also described to play an important role in ovarian carcinoma metastasis.

1.3 Cell adhesion molecules involved in the transcoelomic metastasis of ovarian cancer

Unlike most of other hematogenously metastasizing cancers, ovarian cancer cells are primarily disseminated within the peritoneal cavity and are only superficially invasive. Transcoelomic metastasis, is a multistep process and is directly associated with ascites production (Figure3). It involves shedding of tumor cells from the primary tumor, formation of multicellular aggregates (spheroids), development of resistance to anoikis, peritoneal fluid transportation, implantation into the peritoneum, and their growth as nodules.

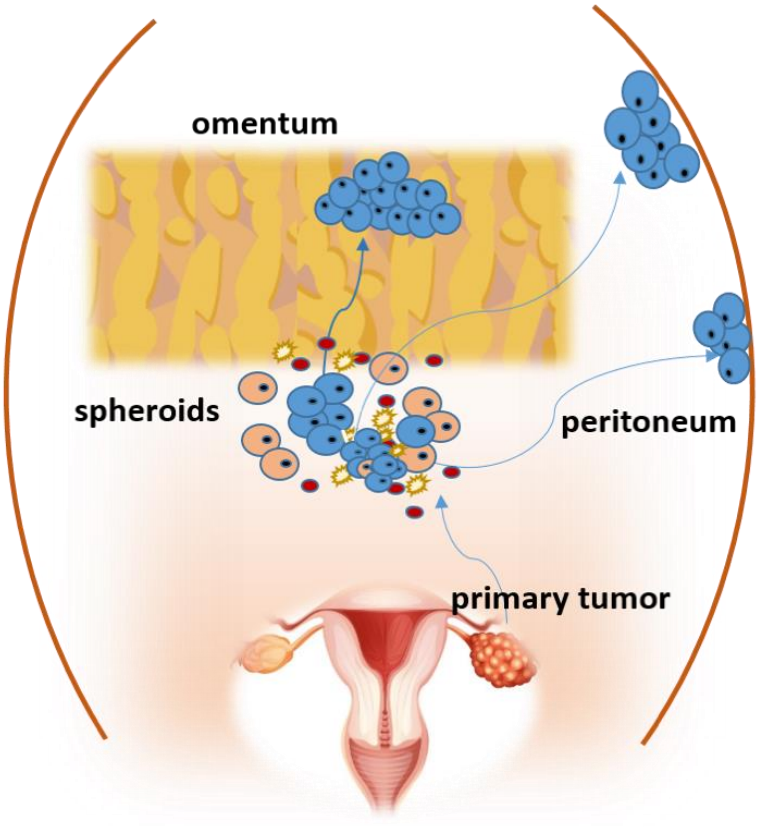

Figure 3 *Transcoelomic Metastasis of Ovarian Carcinoma*

The pivotal role of tumor cell adhesion in cancer dissemination is highlighted by the fact that several cell adhesion molecules (CAMs) are involved in a process of cancer metastasis[95]. Diverse CAMs families are involved in this process, including the cadherins, the integrins, the selectins, and the immunoglobulin superfamily (IgSF). All

major classes of adhesion molecules have been shown to contribute to cancer progression through an individual or overlapping way. Here, the properties of adhesion molecules involved in the metastasis of ovarian cancer would be explained depending on the process of metastasis: detaching from the primary tumor, floating in the abdominal cavity and seeding on the peritoneal sites. Some adhesion molecules are involved in certain steps of the metastasis process, and some of them have overlapping functions at different stages.

1.3.1 Detaching from the primary tumor

Recently, Al Habyan et al. could show using an in vivo ovarian cancer model that spheroids in ascites mainly arise from multicellular detachment from the primary tumor rather than from single cells aggregating within the abdominal cavity. More precisely, cell aggregates in ascites arise from collective dissemination of neighboring cells in the primary tumor and in turn single spheroids developed individual metastatic sites[96]. Epithelial to mesenchymal (EMT) transition and the proteolytic activity were mainly mentioned in the initial detachment before the ovarian carcinoma cells attach and start their metastatic journey. EMT loosens the intercellular adhesions between the cancer cells and eases the attachment of epithelial cells to the basement membrane[97]. One of the critical molecules in epithelial cell-cell adhesion is E-cadherin, a transmembrane glycoprotein localized at the plasma membrane of epithelial cells, which has an extracellular domain involved in cellular adhesion, and an intracellular domain interacting with the actin cytoskeleton to strengthen cell-cell interactions by means of adaptor proteins (eg, α-, and β-catenin). After undergoing EMT, the cells look more like fibroblasts, and acquire an invasive phenotype and proliferate.

Regarding to the proteolytic activity, matrix metalloproteinase (MMP)-2 expressed by the majority of spheroids collected from the ascites, plays an important role in the early metastasis[98] and possibly promotes the fast disaggregation of spheroids on adhesion to the surface of mesothelial cells[99]. Through clustering of collagen binding integrins (α2β1- and α3β1-integrin) on the cancer cell, matrix metalloproteinase (MMP)-9 is induced, which cleaves the E-cadherin ectodomain, contributing to the loosening of cell-cell adhesion and allowing the transformed cells to shed as single cells or spheroids into ascites[100]. Matrix metalloproteinase (MMP)-14 on the tumor

cells cleaves α3-integrin, contributing to the detachment of cells from the primary tumor[101]. MMP14 continues to be expressed on the surface of the spheroids even after they detach from the ovary, since it can be detected in the ascites from the patients undergoing paracentesis.

1.3.2 Floating in the abdominal cavity

During the dissemination of primary tumor cells to the peritoneal cavity, floating mesothelial cells underwent EMT in the presence of ovarian cancer cells secreting TGF-β1, upregulating vimentin and downregulating E-cadherin[102]. Vascular cell adhesion molecule-1(VCAM-1), another important adhesion receptor, is present on mesothelial cells and binds to α4β1-integrin on ovarian carcinoma cells. Function-blocking antibodies directed against vascular cell adhesion molecule-1 and α4β1-integrin block migration and metastasis in a xenograft model[103].

Detached tumor cells float in the ascites as single cells or spheroids until they find a secondary attachment site for further growth. Spheroids floating in ascites have a different phenotype compared with solid primary and metastatic lesions, which provide them an evolutionary advantage in tumor progression. Cells within spheroids are compact with each other and thereby protected from apoptosis and chemotherapy. It has been hypothesized that the spheroids are resistant to anoikis, a specialized form of apoptosis triggered by a lack of attachment to other cells or to the extracellular matrix (EMC), because they highly express B-cell leukemia-xL(Bcl-xL)[104]. A variety of adhesion molecules involved in the spheroids formation and the maintainess of anti-tumor properties: Enhanced expression of α2β1 integrin may influence spheroid disaggregation and proteolysis responsible for the peritoneal dissemination of ovarian carcinoma, indicating a new therapeutic target for the suppression of the peritoneal metastasis associated with advanced ovarian carcinomas[105]. The cells, which expressed more integrin subunits, bind to the components of mesothelium and strengthen the invasive and metastatic potential[106]. Further, disruption of E-cadherin-mediated adhesion and signaling in spheroids using an anti E-cadherin antibody resensitizes ovarian tumor cells to chemotherapy with Taxol[107].

1.3.3 Attach to the secondary site and growth of metastatic lesions

The most common metastatic site of ovarian cancer in the peritoneal cavity is the omentum and peritoneum, both covered with mesothelium[108, 109], which has a smooth and non-adhesive surface that facilitates intracoelomic movement[110]. The mesothelium is formed by a monolayer of mesothelial cells with an underlying basement membrane predominantly composed of collagen types I and IV, fibronectin, and laminin. Fibroblasts and rare and macrophages are interspersed within this membrane and are responsible for producing the matrix proteins[111-114].

It is widely believed that mesothelial cells act as a barrier for cancer cells and represent the first line of defense against ovarian cancer. Ovarian cancer cells can attach directly to the mesothelial cells and impact on the integrity of the mesothelial cell layer, which has been referred to as “mesothelial clearance”[115]. Integrins play an important role in mesothelial cell-cell and cell-ECM adhesions[116], and have been identified as important mediators of ovarian carcinoma metastasis to the mesothelium. Integrin β1[117-119], which can heterodimerize with many different α-integrin subunits, is a key protein regarding the adhesion of ovarian carcinoma to mesothelial cells, as is evidenced by the fact that antibodies against β1-integrin can inhibit this adhesion[120]. Transcriptional up-regulation of the fibronectin receptor, α5β1-integrin due to E-cadherin loss during the EMT process facilitate the adhesion of ovarian carcinoma cells to the secondary site[121]. Other integrin important in spheroids adhesion are α6β1-integrin, which is known to bind laminin, and α2β1-integrin, which binds to type IV collagen[105].

Adhesion of OvCa cells to mesothelial cells is also mediated by different proteases, notably MMP-2, and CD44[118, 122, 123]. After adherence, tumor cells penetrate the mesothelium and subsequently invade the underlying ECM. The cancer cells upregulate MMP2, which then cleaves the ECM components fibronectin and vitronectin into smaller fragments. Then cancer cells can adhere much more strongly to the small fragments (MMP-2–cleaved fibronectin and vitronectin fragments) via fibronectin(α5β1-integrin) and vitronectin (αvβ3-integrin) receptors[114]. CD44 is the principal cell surface receptor for hyaluronic acid. Previous studies have found that the propensity of ovarian carcinoma cells to bind to peritoneal mesothelium can be partly inhibited by a neutralizing anti-CD44 antibody.

Once a metastatic colony is established in the omentum or peritoneum, the ovarian carcinoma cells undergo mesenchymal-to-epithelial transition into an epithelial phenotype, which allows them to respond to paracrine growth factors and sustain fast growth. High proliferation ability would be reactivated after spheroids adhesion to the mesothelium, which is dependent on the initiation of angiogenesis (the formation of new blood vessels from preexisting vasculature). This process is tightly regulated and involves endothelial cell proliferation, differentiation, and migration [124, 125]. The vascular-endothelial-growth-factor- (VEGF-) A, one of the best-characterized proangiogenic molecules, is secreted by the tumor cells and stroma then stimulating the expression and modulates the function of IgCAM members such as ALCAM, ICAM-1, VCAM-1, and PECAM1[126-128]. ALCAM, as a downstream of VEGF, promote the angiogenesis. ICAM-1-mediated adhesion of leukocytes to endothelia is a key event in early angiogenesis and is also important in mediating endothelial cell migration[129, 130]. VCAM-1 is believed to perform a similar role to that of ICAM-1[131], while PECAM-1 regulates both endothelial adhesion and migration by modulating endothelial cell-cell and cell-matrix interactions[132, 133].

2 Material und Methods

2.1 Material

2.1.1 Devices

Table 2 *Devices*

Device	Device designation	Manufacturer
Water bath	GFL 1083	GFL Gesellschaft für Labortechnik, Burgwedel
Microscope	Axiovert 40C	Carl Zeiss AG, Oberkochen
Incubator	Heraeus/Kendro Lab HERAcell Incubator	Heraeus/Kendro Lab, Hanau
Absorption reader	SunriseTM	Tecan Trading AG, Männedorf, Schweiz
Flow cytometer	BD FACSCantoTM II Flow Cytometer	BD Bioscience, San Jose, CA 95131 USA
Centrifuge	Megafuge 1.0R	Heraeus, Hanau
Microcentrifuge	Biofuge FrescoTM	Heraeus, Hanau
Vortex	Vortex-Genie 2	Scientific Industries, Inc., New York, USA
Electrophoresis	HoeferTM SE600 Series Vertical Electrophoresis System	Hoefer, Inc., Holliston, USA
Blotting chamber	HoeferTMTE42 Tank Blotting Unit	Hoefer, Inc., Holliston, USA
Developer	CP1000 Automatic Film Processor	Agfa, Mortsel, Belgien
Power Supply	Electrophoresis Power Supply EPS 601	GE Healthcare Europe GmbH, Freiburg
Camera	Leica DFC320	Leica Mikrosysteme Vertrieb GmbH, Wetzlar
Densitometer	GS-800 Calibrated Densitometer	Bio-Rad, Munich
Precellys Evolution	Precellys Evolution	Bertin Technologies, France

2.1.2 Reagents

Table 3 *Reagents*

Chemicals/Substances	**Manufacturer**
40 % Acrylamid/bis-Acrylamid	Sigma-Aldrich, St. Louis, Missouri, USA
Ammoniumpersulfat (APS)	Bio-Rad, Hercules, Kalifornien, USA
β-Mercaptoethanol	Sigma-Aldrich, St. Louis, Missouri, USA
Blotting-Grade Blocker (Milchpulver)	Bio-Rad, Hercules, Kalifornien, USA
Blottingpaper	Macherey- Nagel, Düren
CozyHi prestained Protein Ladder	highQu GmbH, Kraichtal
Dimethylsulfoxid (DMSO)	Sigma-Aldrich, St. Louis, Missouri, USA
Dulbecco´s Phosphate Buffered Saline (PBS -/-); Modified, without calcium chloride and magnesium chloride, liquid, sterile-filtered, suitable for cell culture	Sigma-Aldrich, St. Louis, Missouri, USA
Dulbecco´s Phosphate Buffered Saline (PBS +/+); With MgCl2 and CaCl2, liquid, sterile-filtered, suitable for cell culture	Sigma-Aldrich, St. Louis, Missouri, USA
Fetal Bovine Serum (FCS)	GIBCO,Invitrogen, Carlsbad, Kalifornien, USA
85 % Glycerin	Carl Roth, Karlsruhe
Immobilon®-P Transfer Membrane	Merck Millipore, Darmstadt
Nonidet® P-40 Substitute	Amresco, Solon, USA
Methanol	ThermoFisher Scientific, Waltham, MA USA
Phosphatase-Inhibitor (50x)	Merck, Darmstadt
Pierce ® BCA Protein Assay, Reagent A & B	ThermoFisher Scientific, Waltham, MA USA
Protease-Inhibitor (100x)	Sigma-Aldrich, St. Louis, Missouri, USA
Rinderserumalbumin (BSA)	Carl Roth, Karlsruhe
Sodiumdodecylsulfat (SDS)	Sigma-Aldrich, St. Louis, Missouri, USA

N,N,N',N'-Tetramethylethylendiamin (TEMED)	Sigma-Aldrich, St. Louis, Missouri, USA
Tricin	Carl Roth, Karlsruhe
Tween 20	Merck, Darmstadt
eBioscience™RBC Lysis Buffer(multi-species)10×	Invitrogen, San Diego, CA, USA
MCDB 105 Medium	Sigma-Aldrich, St. Louis, Missouri, USA
Anti-A,B Mono-Type®reagent	Grifols, Spain
Hematoxylin	Carl Roth, Karlsruhe
Aceton	
Ethanol	Th geyer, Germany
Eosin	
X-ray film developer solution	Calbe Chemie, Germany
X-ray film fixer solution	Calbe Chemie, Germany

2.1.3 Antibodies

Table 4 *Antibody list*

Antibody	**Function**	**Company**
ALCAM NCL-CD166, Mouse mAb IgG2a	Western Blot	Novo Castra Laboratories Ltd, Newcastle, UK, Lot:6034968
E-Cadherin	Western Blot	Cell Signaling Cat.nr. #3195Lot 13
Cytokeratin 7	Western Blot	Dako Cat.nr. M7018 Lotnr. 061(101)
Vimentin	Western Blot	cell Signaling Cat.nr. #5741 Lot1
BCAM	Western Blot	LS Bio#LS-C138475
α-Tubulin (11H10) #2125, Lot:3, Rabbit mAb	Western Blot	Cell Signaling) #2125, Lot:3, Rabbit mAb
BV421 Mouse Anti-Human CD326	FACS	BD Bioscience Cat nr. 563180
PerCP-CyTM5.5 Mouse Anti-Human CD24	FACS	BD Bioscience Cat nr. 561647
FITC Mouse Anti-Human CD45	FACS	BD Bioscience Cat nr. 560976
APC Mouse Anti-Human CD90	FACS	BD Bioscience Cat nr. 561971
Fixable viability stain 575V	FACS	BD Bioscience Cat nr. 565694

2.1.4 Cell lines

SKOV-3 is a human ovarian cancer cell line with epithelial-like morphology. This cell line was established in 1973 from the ascites of a 64-year-old Caucasian female with adenocarcinoma of the ovary. The OAW-42 cell line was established from the ascites of a patient with ovarian cystadenocarcinoma. OVCAR8 was established from a 64-year-old woman ovarian tumor.

2.1.5 Patients material

Ascites was collected from patients diagnosed with advanced-stage serous ovarian carcinoma, after obtaining written informed consent under protocols approved by the Universitätsklinikum Hamburg-Eppendorf, Hamburg, Germany. Ascites was obtained from patients during debulking surgery with primary carcinoma or recurrence.

2.2 Methods

2.2.1 Workflow of ascites-derived cells isolation and culture

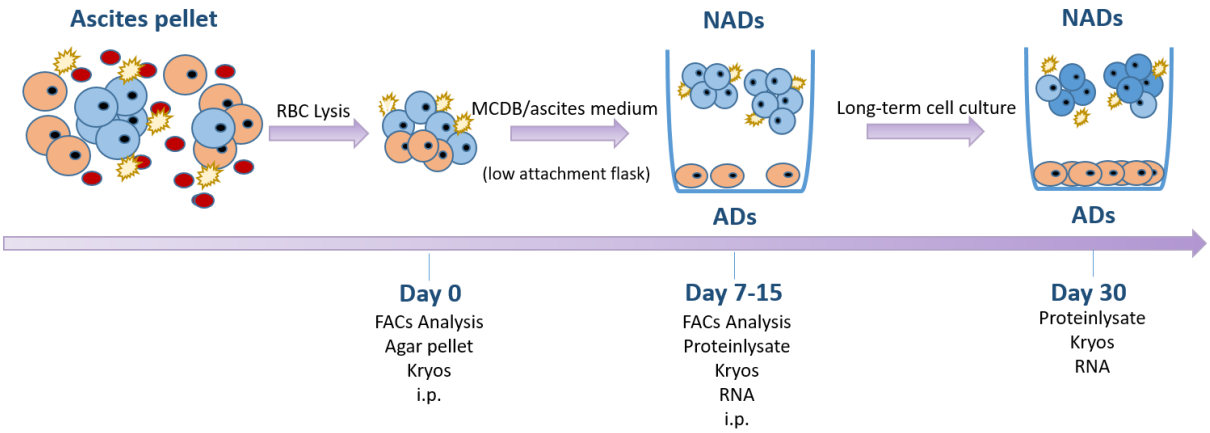

Figure 4 *workflow of ascites-derived cells isolation and culture*

2.2.2 Preparation of Ascites-derived cells of Ovarian Cancer

Patients Ascitic fluid or lavage were collected from debulking. First, centrifuge at 1200rpm speed for 5 minutes at room temperature. The supernatant was collected and used as a cultivation medium for ascites-derived cells. The pellet was resuspended with RBC lysis buffer and incubated for 15 minutes at room temperature. Then, centrifuge at 1200 rpm for 5 minutes. After washing with PBS(+/+) , the original pellet was ready to be further analyzed.

2.2.3 Ascites pellet observation

10 µl of cell suspension were mixed with 10 µl of 0.04% trypan blue. 10 µl mixture were then took into the Neubauer chamber. Different size of the cells and aggregation status were observed under the microscope.

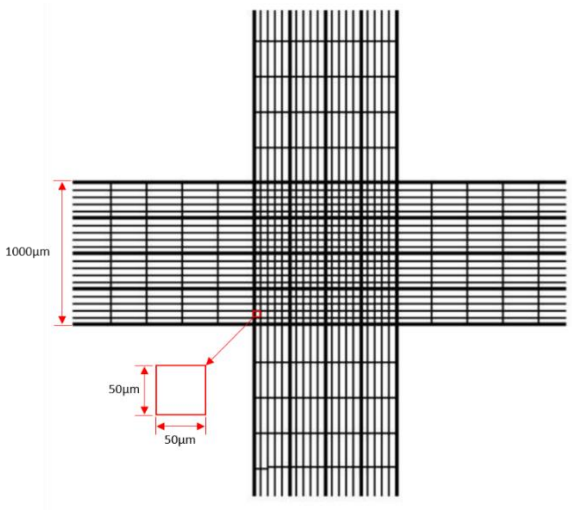

Figure 5 **Hemocytometer (Neubauer chamber)**

2.2.4 Purify the cell aggregates in ascites pellet

To obtain large sized cell aggregates included in the ascites-derived pellet, we use 10µm and 40µm cell strainers. Cells resuspended with PBS++ went through the cell strainer by pipetting or shaking until no liquid in the upper part of the cell strainer was observed. Then PBS++ was added in the cell strainer to flush the cells once more. The <10µm or <40µm fractions were collected in one 50ml tube. Then the cell strainer was turned upside down onto a new 50ml tube and flush back the sample from the cell strainer. The >10µm or >40µm fractions were collected in the new 50ml tube.

2.2.5 Ascites-derived cells culture

MCDB medium preparation: MCDB:DMEM (1:1) growth medium supplemented with fetal bovine serum (10%), glutamine (2 mM) and penicillin/streptomycin (2 mM) (Life Technologies, CA, USA). Additionally, in some cases the clarified supernatant of the ascites was used instead of MCDB as culture medium for ascites derived cells. Cells were maintained at 37°C in the presence of 5% CO_2. In the ascites or MCDB medium, some cells floated as spheroids in the medium (non-adherent cells, NADs) while some cells attached to low attachment plates (adherent cells, ADs).

2.2.6 Passage the primary isolated ascites derived cells

The NADs were collected and then washed with PBS (-/-). The adherent cells were detached from the bottom of the cell culture flask by addition of 1x trypsin and a maximum incubation for 5 minutes at 37 ° C in the incubator. The ADs were then added

to a 15 ml tube after adding double volume of MCDB or ascites medium. Falcon transferred and centrifuged (5 minutes, 1200 rpm, RT). The cell pellet was taken up in an appropriate amount of medium and seeded in a new low attachment plate.

2.2.7 Cell counts

10 µl of cell suspension were mixed with 10 µl of 0.04% trypan blue (1: 1) and filled in a Neubauer counting chamber. The cells in four squares were counted (Diaphot 300 Phase Contrast Inverted Microscope from Nikon) and cell amount was calculated as follows:

$$\text{Particles per ml volume} = \frac{\text{counted particles}}{\text{numbers of counted squares}} * 2\ (\text{Dilution factor}) * 10^4\ (\text{Charmber factor})$$

2.2.8 FACS analysis

Table 5 *FACS samples preparation*

	1%BSA/ PBS	AB blocking	CD45	EpCAM	CD24	CD90	FVS	Total volume
control	80µL	20 µL	-	-	-	-	-	100 µL
Multi-stained	72.4 µL	20 µL	5 µL	1 µL	1 µL	0.8 µL	0.8 µL	100 µL

After washed with 500 µl PBS (+/+) (centrifugation: 1500 rpm/5 min/4°C), the cell pellet (around 500,000 cells) were resuspended in 100 µl antibody solution. All antibodies used were diluted in 1% BSA/PBS(+/+) and AB blocking solution (Table 5). The multi-stained samples were incubated with the multiple antibodies solution (Table 5), while control samples only incubated with 1% BSA/PBS(+/+) and AB blocking. All samples were incubated for 30 minutes at 4°C in the dark. 500 µl PBS(+/+) was directly added to each tube after incubation(centrifuging at 1500 rpm/5 min/4°C). Then the pellets were resuspended with 500 µl 3.7% formalin fix buffer. The samples were measured on the BD FACSCanto™ II Flow Cytometer (core facility, UKE). The evaluation was carried out with the Flowjo software.

2.2.9 Protein extraction from ascites derived cells

ADs and NADs were collected separately. The NADs supernatant were collected and then centrifuge at 1200rpm, RT, for 5min. NADs pellet was ready after washing with PBS (-/-) and centrifuged at 1200rpm, RT, for 5min. ADs were washed with PBS (-/-) and digested with trypsin for 5 min. The detached ADs were then added to a 15 ml tube with double volume of MCDB medium. Centrifuge at 1200rpm, RT, for 5min. ADs pellet was ready after washing with PBS (-/-) and centrifuged at 1200rpm, RT, for 5min. The appropriate amount of RIPA buffer (65 mM Tris, 154 mM NaCl, 1% Nonidet® P-40 substitutes, 1% Na deoxycholate, 1 mM EDTA, pH 7.4) + 1x protease inhibitor (100x) + 1x phosphatase Inhibitor (50x) was added to the ADs and NADs pellet. This step was done on ice. The cell-RIPA mixture was incubated on ice for 30 minutes and mixed vigorously (vortex) every 10min. After centrifuging for 5 minutes at 4 °C and 13,000 rpm, the supernatant was transferred to a new 1.5 ml eppendorf tube and stored at -80°C.

2.2.10 Protein extraction from tumor material

10μm sections were cut from cryo-tumor material and HE staining was performed. The tissue was tailored if necessary to obtain at least up to 50% invasive tumor cells in the sample used for protein extraction. Approximately 10 sections, 30μm-thick, were collected in RIPA(+/+) buffer and homogenized using a micro-dismembrator (Precellys Evolution, Bertin Technologies) (6400 rpm, 3x 30 seconds, 30 seconds break in between). The bubbles on the top were removed after centrifuging at 13000rpm for 1 minute and the protein solution then transferred to a new tube. After centrifugation at 13000rpm for 5 minutes at 4°C, the supernatant were collected as protein lysis.

2.2.11 Protein estimation BCA

The determination of the protein concentration for the immunological detection of proteins was done according to the BCA method. In the BCA method, it comes to the so-called biuret reaction. The protein forms a complex with Cu2 + ions. The Cu2 + ions are subsequently reduced to form a violet color complex with bicinchoninic acid (BCA). For this purpose, the samples to be determined were diluted 1: 5 with 50 mM Tris buffer. The protein standard is bovine serum albumin (BSA). Seven different BSA

concentrations were prepared by dilution with RIPA buffer and Tris / HCl (50 mM) (see Table 13). From each sample 25 µl protein lysate was taken in a well of a 96-well plate for the measurement. 200 µl of the BCA working solution (solution A: solution B in the ratio 50: 1) were pipetted into each sample. After incubation for 30 minutes at 37°C, the photometric measurement at 540 nm was performed with the SunriseTM and Magellan V6.6 software (Tecan Trading AG).

Table 6 *BCA standard preparation*

Number	BSA-concentration in µg/ ml	BSA µl	Lysis buffer (RIPA) µl	Tris/ HCl µl
1	1000	500 aus Stammlösung	200	300
2	750	375 aus Stammlösung	200	425
3	500	500 aus (1)	100	400
4	250	500 aus (3)	100	400
5	125	500 aus (4)	100	400
6	62,5	500 aus (5)	100	400
7	31,25	500 aus (6)	100	400
8	Blank	-	20	80

2.2.12 HE staining for tumor cryos sections

Tissue sections were rinsed in aceton for 5 minutes, then in distilled water for 5 minutes twice. Nuclei staining was performed in hematoxylin solution for 5 minutes, then rinsed in distilled water. Then the sections were stained with eosin solution for 5 min, followed by dehydration with graded alcohol (80%-96%-100% Ethanol) and cleared in xylene for 5 minutes twice. The mounted slides were then examined and photographed.

2.2.13 Western blot

2.2.13.1 Electrophoretic Separation of Proteins (SDS-PAGE)

The separation of proteins was carried out by means of discontinuous polyacrylamide gel electrophoresis according to the principle of L. Ornstein and B.J. Davis (Ornstein et al., 1964). Polyacrylamide gels consisting of a stacking gel (5%) and a separating gel (8%) were used (composition see Table 14). For the separation, 20 µg of protein were adjusted to a volume of 30 µl with RIPA buffer (65 mM Tris, 154 mM NaCl, 1% Nonidet P-40, 1% Na deoxycholate, 1 mM EDTA, pH 7.4) and then mixed 1: 1 with PCsb2 denaturation buffer (1 g sucrose, 1 ml 0.5 M Tris buffer (pH 6.8), 4 ml 10% SDS, 1-2 mg bromophenol blue, 3.5 ml distilled water, 1 , 5 ml of β-mercaptoethanol). The mixture was denatured for 5 minutes at 95 ° C and applied to the gel. The protein molecular weigth standard was the CozyHi prestained Protein Ladder from HighQu. The gel run was aprox.19 hours and 30 minutes at 58 V using the HoeferTM SE600 Series Vertical Electrophoresis System.

Table 7 *SDS-PAGE recipe*

Components	**Separating gel**	**Collection gel**
87% Glycerin	8 g	-
Aqua dest.	20 ml	11,9 ml
3x Gelpuffer mit SDS	20 ml	4,7 ml
40 % AA/BAA	12 ml	2,3 ml
APS 10 %	300 µl	225 µl
TEMED	30 µl	25 µl

Following buffer solutions were used for electrophoresis:

1x cathode buffer (10x: 121.14 g Tris, 179.2 g Tricine, make up to 1 L with distilled water pH 8.25)

1× anode buffer (10x: 242.28 g Tris, make up to 1 L with distilled water pH 8.9)

3x gel buffer with SDS: 181.7 g Tris, fill up to 0.5 L with distilled water, pH 8.45, add 15 mL 10% SDS before use.

0.5 M Tris buffer:6.05 g Tris, fill up to 100 mL with distilled water, pH 6.8

2.2.13.2 Blotting and Immunological detection of proteins

After separation of the proteins in the polyacrylamide gel, the transfer was carried out on a PVDF membrane. After activation of the membrane with methanol, the transfer took place in 1x transfer buffer (10x: 121.41 g Tris, 144.89 g glycine, replenish to 1 L with distilled water) for 6 h at 400 mA. This followed by the blocking of the membrane for one hour at the room temperature in a 5% milk powder solution (5g blotting-grade blocker+100 ml 0.05% TBS-T) and incubated with the primary antibody overnight at 4°C. After washing 3 times with 0.05% TBS-T (100 ml 10x TBS, 5 ml 10% Tween20, making up to 1 liter with distilled water) for 10 minutes at RT on the shaker, the membrane was incubated for one hour with the secondary antibody. The membrane was then washed 3 times for 10 minutes at RT on the shaker with 0.05% TBS-T. Antibodies were detected using Westar Nova 2.0 Chemiluminescent Substrate for Western Blotting Kit from Cyanagen.

Table 8 *Antibodies used and associated dilutions for Western blot analysis*

Primary Antibody	**Dilution**	**Secondary antibody**	**dilution**
ALCAM NCL-CD166, Lot:6034968	1:400 in 1,5% Milk in TBST	Anti-Mouse sc-2055, Lot:F2413	1:8000 in 1,5% Milk in TBST
α-Tubulin CellSignaling#2125, Lot:3	1:10000 in 5% BSA in TBS-T	Anti-Rabbit sc-2054, Lot:E1713	1:8000 in 1,5% Milk in TBST
E-Cadherin cell Signaling Cat.nr. #3195 Lot 13	1:2000 5% BSA in TBST	goat anti -rabbit IgG-HRP	1:8000 1,5% Milk in TBST
Cytokeratin 7 Dako Cat.nr. M7018 Lotnr. 061(101)	1:2000 in 5% Milk in TBST	goat anti mouse sc-2005, Lot: G1213	1:8000 1,5% Milk in TBST
Vimentin cell Signaling Cat.nr. #5741 Lot1	1:2000 5% BSA in TBST	goat anti -rabbit IgG-HRP	1:8000 1,5% Milk in TBST
BCAM LS Bio#LS-C138475	1:5000 blocking reagent	goat anti -rabbit IgG-HRP	1:8000 1,5% Milk in TBST

Following solutions were used for blotting or during protein detection:

10x TBS:

24.22 g of tris, 80.06 g of NaCl, fill up to 1 L with distilled water.

10% Tween 20:

5 g Tween20, fill up to 50 ml with distilled water.

X-ray film developer:

X-ray film developer solution part 1,2 and 3, fill up to 2.5 L with distilled water.

X-ray film fixer:

X-ray film fixer solution part 1 and 2, fill up to 2.5 L with distilled water.

2.2.14 Reblot

The membrane was washed twice with 0.05% TBS-T followed by twice water washing. Reblot Plus Mild Antibody Stripping Solution from Merck Millipore (1:10 in distilled water) was used 25 minutes at RT. Then, membraned was blocked with 5% milk powder solution (5 g blotting-grade blocker + 100 ml 0.05% TBS-T) for 60 minutes at RT or overnight at 4°C. Furthermore, the immunological detection of proteins was performed as described before.

2.2.15 Quantitative analysis of the western blot results

The films were scanned under the Densitometer, then the intensity of each band was measured. The value from each band was normalized with positive control and housekeeping gene. Band intensities were quantified by densitometry (GS-700 Imaging Densitometer, Bio-Rad, Hercules, California) and calculated as percent-intensity of SKOV3 (set as 100%) after correction for equal α-Tubulin/β-Actin loading. The optical densities of bands were quantified separately as well as together and calculated in relation to the targeted band in SKOV3.

3 Results

In order to identify molecular components that characterize ascites-derived tumor cells and to compare to those tumor cells from primary and metastatic tissue, following studies were carried out:

(i) the morphology of cells derived from ascites were documented from different time points: on the first day and after culturing for several days;

(ii) the expression of several adhesion molecules in cultured ascites-derived cells were analyzed by western blot;

(iii) FACS (Fluorescence-activated Cell Sorting) was applied for screening ascites-derived cells for tumor and non-tumor cell populations in a more efficient way, given the high diversity between different samples;

(iv) Adhesion molecules were detected in matched pairs of ascites-derived cells and primary/metastasis tumor (same patients).

3.1 Morphology of Ascites-derived cells in OvCa Patients

The morphological features of ascites-derived cells from OvCa patients (n=42) were assessed by phase contrast microscopy immediately after collection on Day0. Here, we observed very heterogeneous patterns between the samples collected from different patients. Ascites derived cells presented as three main components, which are only small singe cells (n=19), little amount of spheroids with big amount of single cells (n=14) and mainly consisted of spheroids (n=9). Strainers of 10µm and 40µm were frequently used for separating the original pellet into different fractions. The multicellular aggregates (spheroids) were mainly collected in 10-40µm and >40µm fractions, while <10µm fraction only consisted of small single cells (figure 6A).

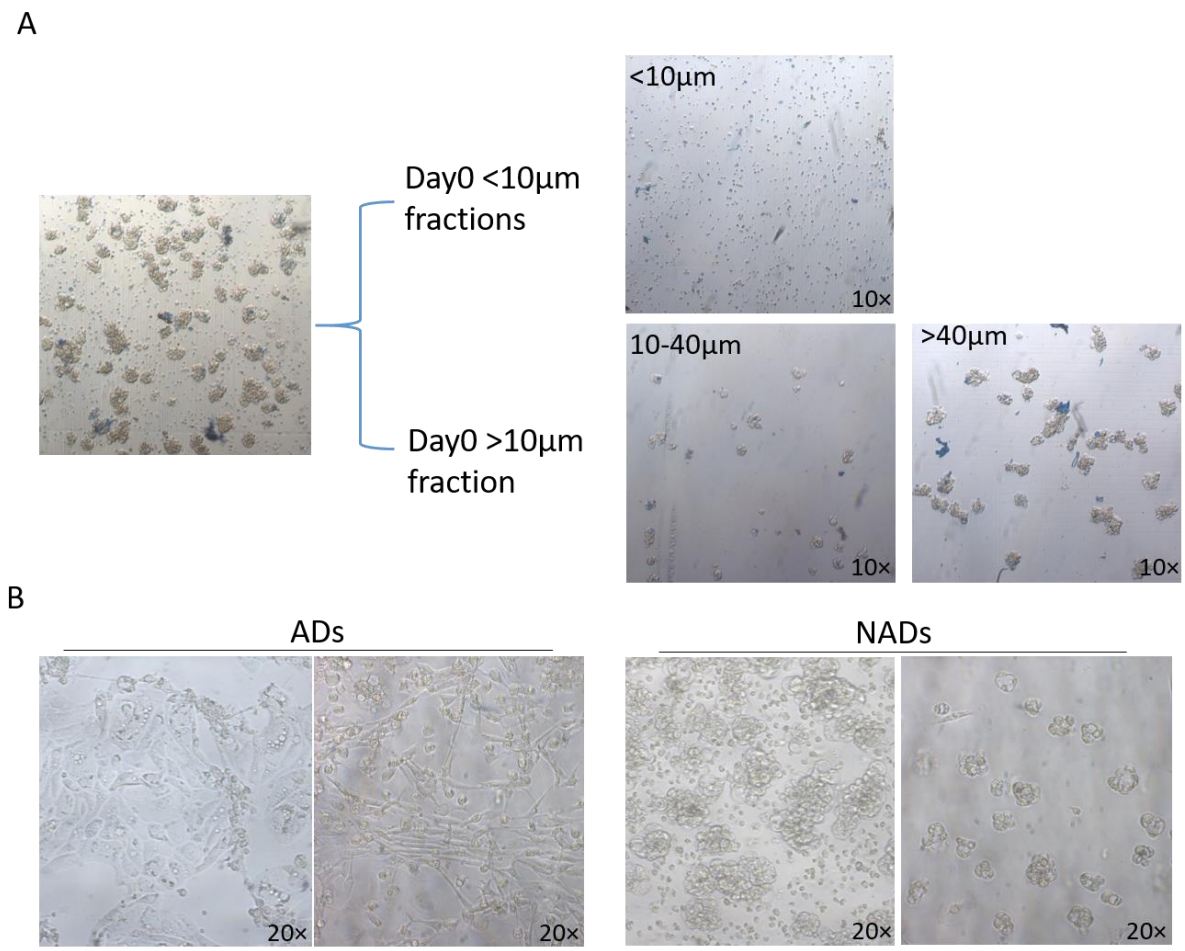

Figure 6 *Morphology of multi-sized fractions from ascites-derived cell, ADs and NADs*

A, Day0 original pellet were separated into <10µm, 10-40µm and >40µm fractions.
B, Morphological features of ADs and NADs seeded on low-attachment plate. The images are representatives of (n = 35) samples.

After several days cultured in low-attachment plates with ascites or MCDB medium, two main populations were observed: elongated spindle-shaped mesenchymal-like or cobblestone-shaped epithelial-like cells adhered to the low-attachment plate (ADs); multicellular aggregates (spheroids) and small single cells were floating in the supernatant without attachment (NADs) (figure 6B).

The majority of ADs formed in <40µm fractions, while only small amount in >40µm fractions. ADs presented more frequently as elongated spindle-shaped mesenchymal-like morphology than cobblestone-shaped epithelial-like morphology (figure 6B). ADs showed high proliferation during culture, especially in ascites medium.

In NADs, considerable variations were noted in the morphology, size and number of spheroids from different patients as well as a high range of sizes within the same patient (figure 6B). The spheroids were not only in the form of compact balls, but also displayed unformed clusters with loose aggregates in some samples. NADs presented low-proliferation during culture independently of the medium used (MCDB medium or ascites medium).

3.2 Differential expression of adhesion molecules and EMT markers in ADs and NADs

The comparative expression analyses in ADs and NADs were performed by western blot using specific antibodies for E-Cadherin, vimentin and ALCAM. E-Cadherin and cytokeratin7 are epithelial makers, and vimentin is a mesenchymal marker. Additionally, ALCAM (Activated Leukocyte Cell Adhesion Molecule) and E-Cadherin are cell–cell adhesion molecules.

As shown in Figure 7, E-Cadherin is higher expressed in NADs compared to the corresponding ADs in each patient. Vimentin showed an opposite expression pattern, with lower expression in NADs than in ADs in all 6 samples. The expression of cytokeratin7 was also higher in NADs than in ADs in 5 samples. However, no definite differences in ALCAM expression between ADs and NADs were observed. Quantitative values were shown in Figure 7B.

A

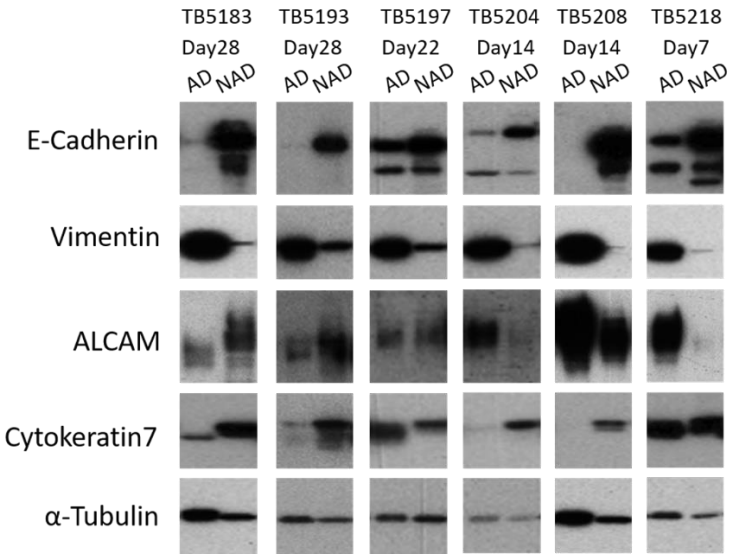

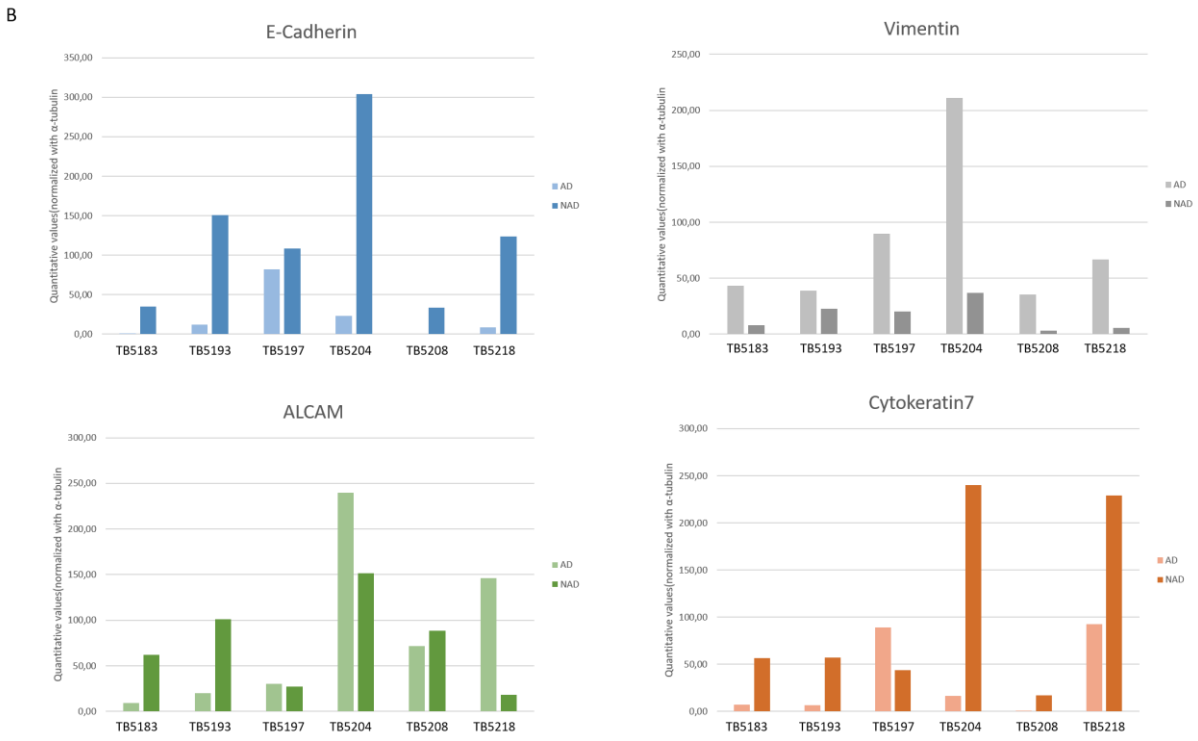

Figure 7 *Expression analysis of E-Cadherin, Vimentin, ALCAM and Cytokeratin7 levels in ADs and NADs by western blot*

A, ADs and NADs derived from different OvCa patients from different time point by western blot;

B, Quantitative values of western blot

E-Cadherin, Cytokeratin7 and ALCAM expression levels showed a wide range among the 6 samples in western blot, suggesting variable expression levels of these molecules in different patients as well as in cells from the same origin but cultured under different media conditions or during a long-term culture period. Reduced E-Cadherin expression were observed in some NAD cells after 28 days culture in comparison with those from Day7. Moreover, higher expression of E-Cadherin was found when ascites-derived cells were cultured in ascites medium compared to MCDB medium (results not show). In some samples no E-Cadherin expression were found in both ADs and NADs after culturing for a long period, but it is unknown whether cells expressed no E-Cadherin at all even at the beginning or E-cadherin expression is down-regulated after long-term culturing.

Contrary to our expectations, adherent cells showed a more mesenchymal phenotype with higher vimentin and lower E-cadherin levels than non-adherent floating cells. The unexpected strong differences regarding the EMT expression pattern in ADs and NADs led us to the question about the cellular components of these two populations and their tumoral/non-tumoral properties. Therefore, in a further step we screened the cellular composition of the ascites-derived cells at the beginning and also after long-term culture with a more efficient way using flow cytometry.

3.3 Assessment of Cell Surface Markers by FACS

To further understand the components of ascites-derived cells, FACS (Fluorescence-activated Cell Sorting) analysis was done with an established antibody panel: CD45 (immune cells marker), CD24/EpCAM (tumor markers) and CD90 (mesothelial-like cell marker). Table 9 shows the patients characteristics of 15 samples measured by FACS, including age at diagnosis, FIGO stage, corresponding TNM-classification, histology and lymph node status (Table9). The ages at diagnosis ranged from 40 to 79 years old. FIGO stages are ranging from IIB to IVA. 8 patients were FIGO IIIC and others were distributed in FIGO IIB, IIIB and IVA. The histology of the analyzed patients was mainly HGSC (high-grade serous carcinoma), except one which showed an endometrioid histology. Lymph node metastasis were found in 8/15 patients.

Table 9 *Clinical characteristics of patients from FACS analyzed ascites-derived cells (n=15)*

TB Nr.	Age	FIGO	Histology	TNM	LN
TB5218	72	IIIC	HGSC	pT3c	1
TB5349	59	IIIC	HGSC	pT3c	1
TB5354	74	IIIC	HGSC	pT3b	0
TB5359	40	IIIB	HGSC	pT3b	0
TB5399	79	IIB	endometrioid	pT2b	0
TB5400	70	IIIC	HGSC	pT3c	1
TB5415	68	IIIC	HGSC	unknown	unknown
TB5420	65	IIIC	HGSC	pT3c	1
TB5424	71	IVA	HGSC	pT3c	1
TB5437	65	IIIC	HGSC	pT3c	1
TB5445	56	IIIB	HGSC	pT3b	1
TB5502	63	IIIC	HGSC	pT3c	1
TB5508	74	IIIB	HGSC	pT3b	0
TB5510	75	IVA	HGSC	unknown	unknown
TB5513	78	unknown	HGSC	pT3b	0

Abbreviations: FIGO, International Federation of Gynecology and Obstetrics; HGSC, High Grade Serous Carcinoma; LN, Lymph node metastasis (1, had lymph node metastasis; 0, had no lymph node metastasis).

3.3.1 Components of ascites-derived cells on day0

After excluding the dead cells which showed a positive staining for fixable viability stain 575V, variable expression levels of the four markers mentioned before, were observed in 11 samples on day0: CD45+(90.5%±10.4%), CD90+(7.2%±7.0%), CD24+(41.4%±26.3%), and EpCAM+(7.2%±10.2%) (mean±standard deviation, Figure 8). The CD45+ cells represented the biggest part of the whole population in all samples, followed by CD24+ cells. A relatively low amount of CD90+ and EpCAM+ cells were detected in most samples (10/11), however a high heterogeneity regarding the content of CD90+, CD24 +and EpCAM+ cells was observed among samples (Figure 8)

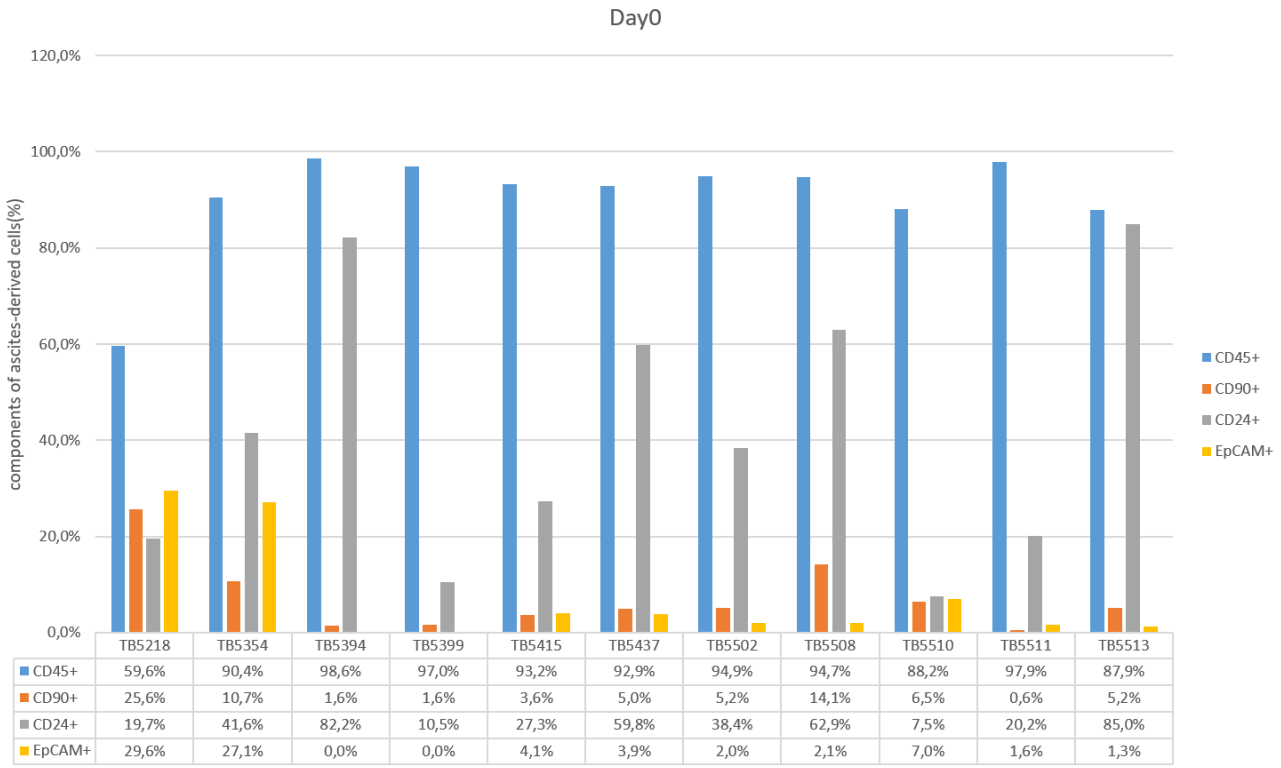

	TB5218	TB5354	TB5394	TB5399	TB5415	TB5437	TB5502	TB5508	TB5510	TB5511	TB5513
CD45+	59,6%	90,4%	98,6%	97,0%	93,2%	92,9%	94,9%	94,7%	88,2%	97,9%	87,9%
CD90+	25,6%	10,7%	1,6%	1,6%	3,6%	5,0%	5,2%	14,1%	6,5%	0,6%	5,2%
CD24+	19,7%	41,6%	82,2%	10,5%	27,3%	59,8%	38,4%	62,9%	7,5%	20,2%	85,0%
EpCAM+	29,6%	27,1%	0,0%	0,0%	4,1%	3,9%	2,0%	2,1%	7,0%	1,6%	1,3%

Figure 8 *Cellular composition of ascites samples in 11 OvCa patient samples assessed by FACS at day 0*

3.3.2 Characteristics of ADs and NADs

Similarly, a second FACS was performed in ADs and NADs after a few days culturing in low-attachment plates. Within the viable cells two populations were observed: one is a $CD45^{-}CD90^{+}CD24^{-}EpCAM^{-}$ population, where cells only express CD90, without expression of CD45, CD24 and EpCAM; another one is $CD45^{-}CD90^{-}CD24^{+}EpCAM^{+}$ population, where cells expressed CD24 as well as EpCAM without expression of CD45 and CD90.

Most ADs grown from small fractions (<40 μm), therefore we assume that these cells probably were present in the whole pellet as single cells and not included in cell aggregates structures. Interestingly, $CD45^{-}$**$CD90^{+}$**$CD24^{-}EpCAM^{-}$ population were mainly gathered in ADs (60.3%±17.3%) (Figure 9A, 9C and 9D) in comparison to NADs (11.8%±14.4%). In contrast, a higher number of $CD45^{-}CD90^{-}$**$CD24^{+}EpCAM^{+}$** cells were detected in NADs (7.6%± 8.9%), than in ADs (0.6%±1.1%) (Figure 9B, 9E, 9F). Both ADs and NADs contained a large population of $CD45^{+}$ cells (Figure 9C and 9E). Notably, the amount of $CD45^{+}$ cells were getting reduced during cell culture when comparing cultured ADs/NADs to the original pellet at Day0 (Figure 9C, 9E and 9C).

A

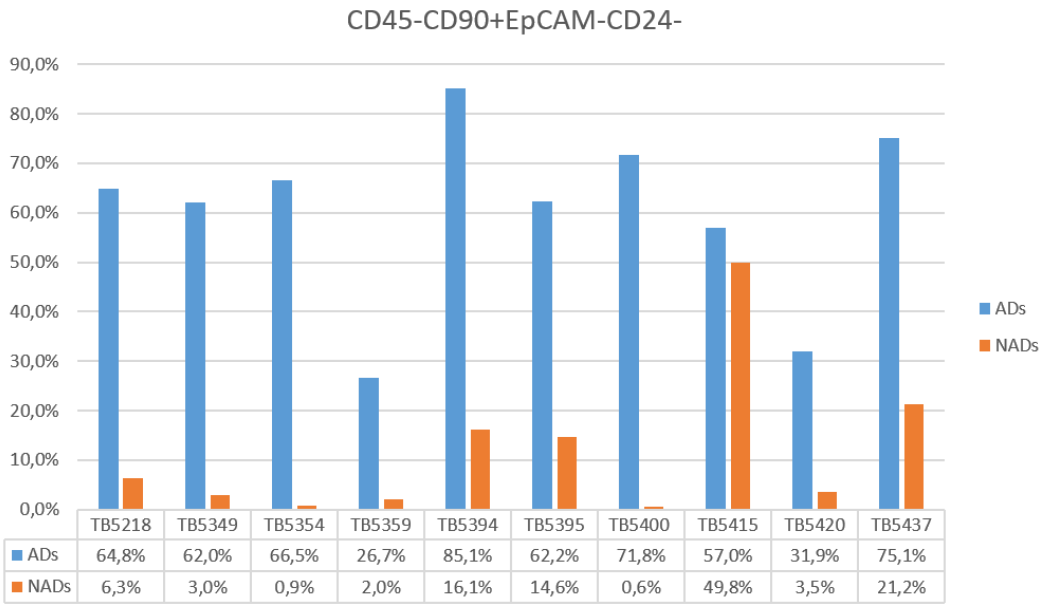

	TB5218	TB5349	TB5354	TB5359	TB5394	TB5395	TB5400	TB5415	TB5420	TB5437
ADs	64,8%	62,0%	66,5%	26,7%	85,1%	62,2%	71,8%	57,0%	31,9%	75,1%
NADs	6,3%	3,0%	0,9%	2,0%	16,1%	14,6%	0,6%	49,8%	3,5%	21,2%

B

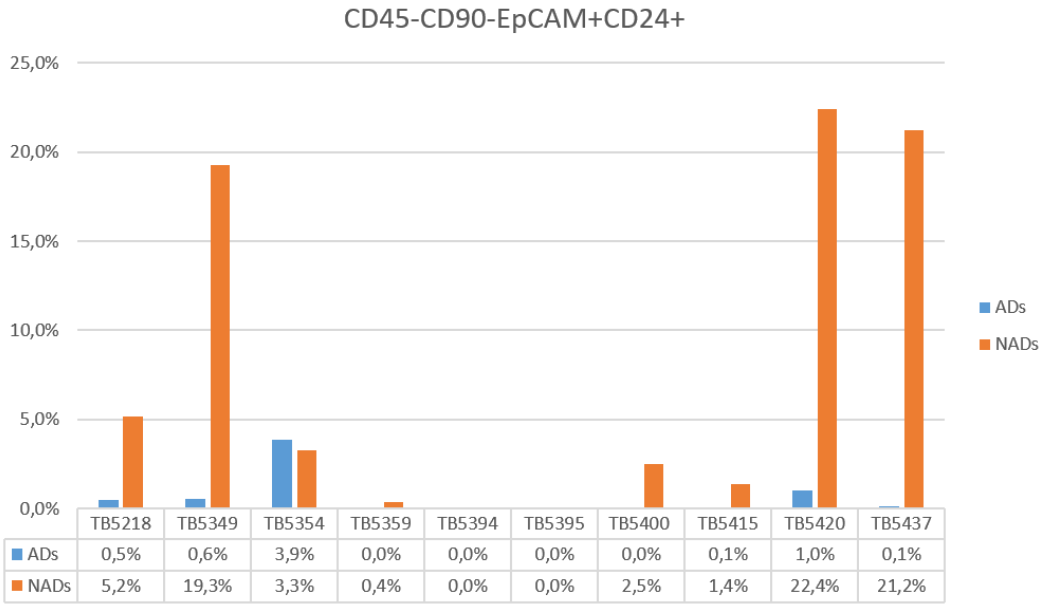

	TB5218	TB5349	TB5354	TB5359	TB5394	TB5395	TB5400	TB5415	TB5420	TB5437
ADs	0,5%	0,6%	3,9%	0,0%	0,0%	0,0%	0,0%	0,1%	1,0%	0,1%
NADs	5,2%	19,3%	3,3%	0,4%	0,0%	0,0%	2,5%	1,4%	22,4%	21,2%

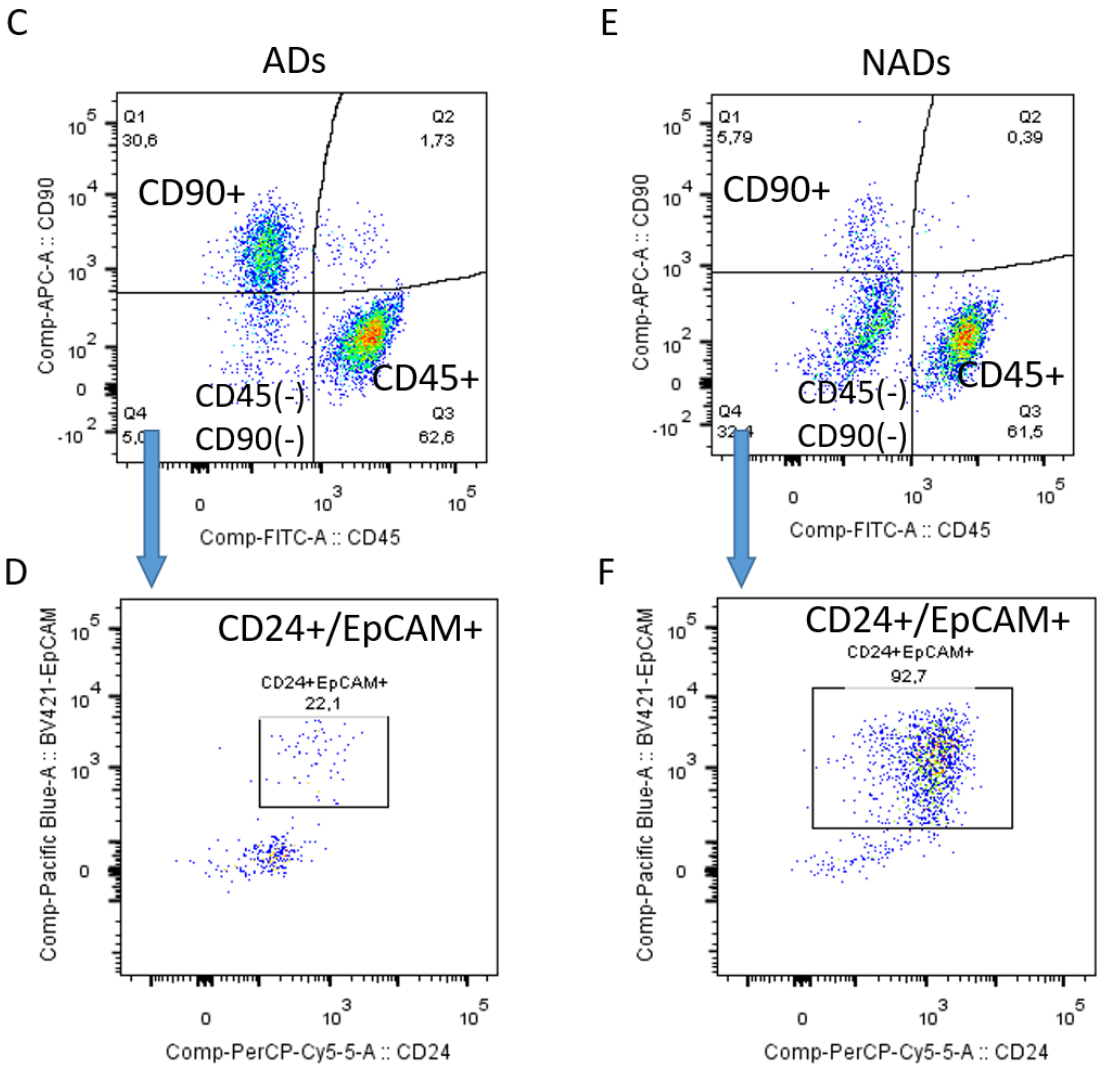

Figure 9 *FACS analysis in ADs and NADs*

A, $CD45^{-}CD90^{+}CD24^{-}EpCAM^{-}$ population in ADs and NADs;

B, $CD45^{-}CD90^{-}CD24^{+}EpCAM^{+}$ population in ADs and NADs;

C-F, a representative analysis from one sample;

C and E, CD45 and CD90 expression in ADs and NADs;

D and F, expression of CD24 and EpCAM in the CD45-CD90- population.

3.3.3 Purifying NADs from ascites-derived cells

CD24 and EpCAM expression were mainly found in NADs, rather than in ADs. The morphology of NADs were primarily cell aggregates (spheroids) which are bigger than other single cells. Therefore, cell strainers were used as a supportive tool to enrich the original pellet with cell aggregates (spheroids).

The size of 10µm and 40µm were used in order to separate the original pellet into different fractions. Different sizes of cell strainers were chosen depending on the size of spheroids. The size of 10µm cell strainers were used in the first three samples which has smaller spheroids (Figure 10A, B). The other 5 samples were filtered by the size of 40µm cell strainer which contained bigger spheroids (Figure 10A, B).

To the aim of evaluating the effect of using cell strainers, two populations: $CD45^+/CD90^+CD24^-EpCAM^-$ and $CD45^-CD90^-CD24^+/EpCAM^+$ were compared between the small fraction and big fraction. Generally, the small fraction expressed more (42.6%±29.1%) $CD45^+/CD90^+CD24^-EpCAM^-$ than big fractions (26.2%±25.6%), as well as less expression (12.5%±8.6%) of $CD45^-CD90^-CD24^+/EpCAM^+$ compared to big fractions (30.9%±26.2%) (Figure10A, B). More precisely, in 4/8 samples, much more $CD45^+/CD90^+CD24^-EpCAM^-$, as well as much less $CD45^-CD90^-CD24^+/EpCAM^+$ were detected in small fractions than in big fractions. However, opposite expression pattern or no obvious differences were detected in other 4/8 samples. Figures 10C-F show a representation from one of the samples, which showed different populations screened by FACS.

A

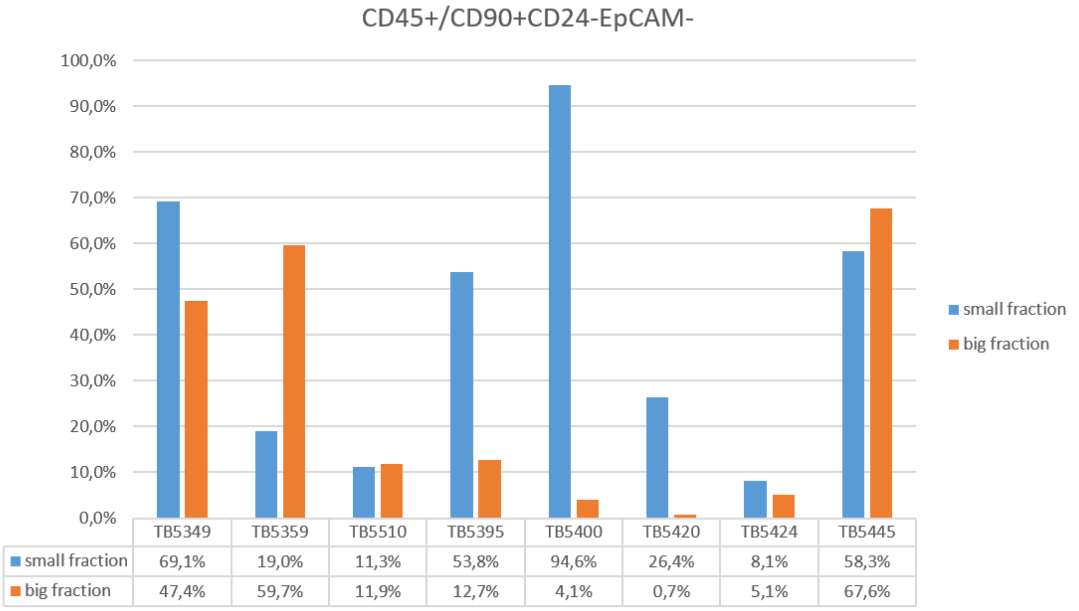

	TB5349	TB5359	TB5510	TB5395	TB5400	TB5420	TB5424	TB5445
small fraction	69,1%	19,0%	11,3%	53,8%	94,6%	26,4%	8,1%	58,3%
big fraction	47,4%	59,7%	11,9%	12,7%	4,1%	0,7%	5,1%	67,6%

B

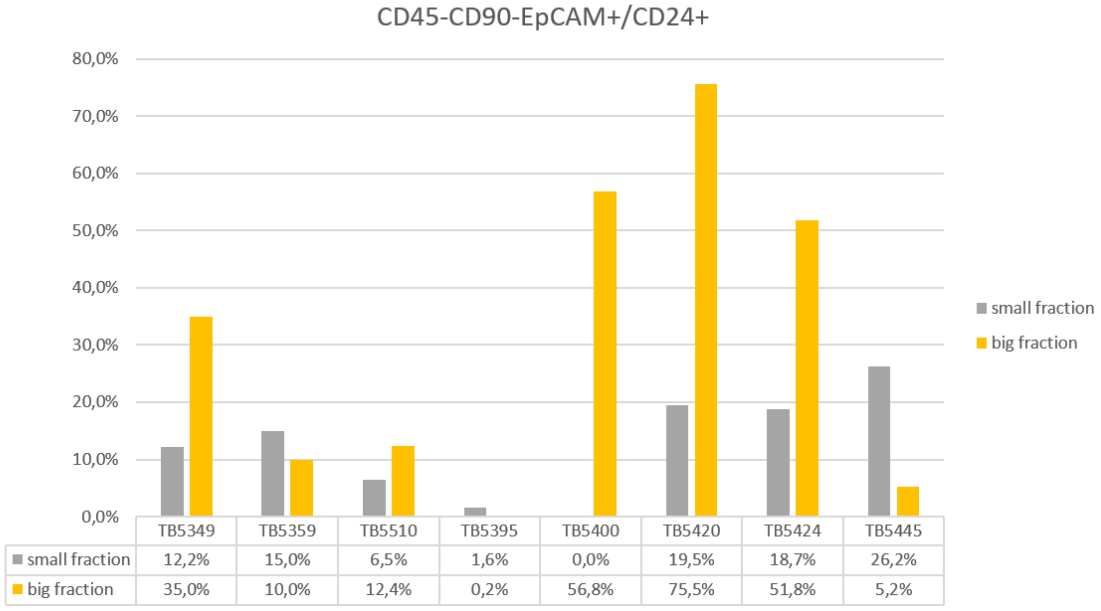

	TB5349	TB5359	TB5510	TB5395	TB5400	TB5420	TB5424	TB5445
small fraction	12,2%	15,0%	6,5%	1,6%	0,0%	19,5%	18,7%	26,2%
big fraction	35,0%	10,0%	12,4%	0,2%	56,8%	75,5%	51,8%	5,2%

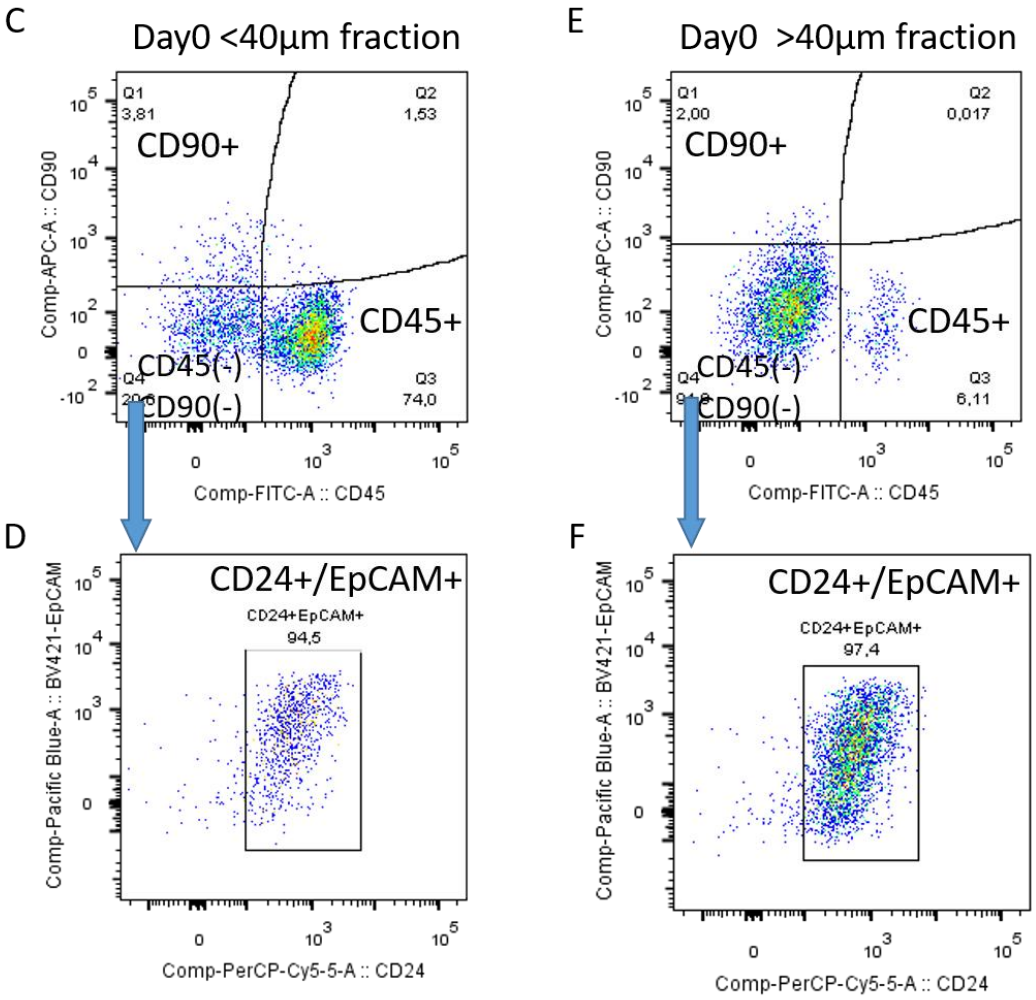

Figure 10 *FACS analysis in ADs and NADs.*

A, percentage of $CD45^{+}CD90^{+}CD24^{-}EpCAM^{-}$ population in ADs and NADs;

B, percentage of $CD45^{-}CD90^{-}CD24^{+}EpCAM^{+}$ population in ADs and NADs;

C-F is a representation from one of the samples;

C and E, CD45 and CD90 expressions in ADs and NADs;

D and F, expression of CD24 and EpCAM in $CD45^{-}CD90^{-}$ population.

3.4 Adhesive molecules expressed in ascites-derived cells and tumor

NADs contained high expression of E-Cadherin and low expression of Vimentin compared to ADs as we showed in western blot. FACS results further confirmed the majority of CD24 and EpCAM positive populations were in NADs, and ADs mainly expressed CD90. Therefore, we further focused our attention on NADs. In order to figure out potential differences in the expression of adhesive molecules in spheroids and in tumor tissues. Both peritoneal carcinoma tissue samples and ascites were collected from the same patients.

3.4.1 Screening of tumor materials derived from OvCa patients

In addition to the ascites-analysis, tumor material were analyzed from patients whose NADs expressed high level of E-Cadherin and low level of vimentin. Clinical characteristics and tumor properties are shown in table 10. In total, 4 pairs were available for the analysis. 3 of them were HGSC (High-Grade Serous Carcinoma) patients, 2/3 were FIGO IIIC and 1/3 was FIGO IVA. All 4 patients had lymph node metastasis. Primary tumor sites of 2 patients were from the fallopian tube, and 2 from the ovary. The specimen's sites were omentum (2/4) or ovary (1/4). With regard to tumor histology, the amount of tumor varied a lot between the 4 specimens, which was quantified by Hematoxylin and eosin staining and evaluation under the microscope (Figure 11). Three of them contained more than 60% tumor, and one specimen showed only 10% tumor inside. Cryo-sections were collected for tumor protein isolation for the further analysis.

Table 10 *Description of patients recruited for tumor isolation (n=4)*

Patient number	T Nr.	Age	FIGO	Histology	LN	Stage	Primary tumor site	Specimen site	Tumor %
1	T7110	56	IIIC	HGSC	1	pT3c	fallopian tube	omentum	60%
2	T7114	61	IVA	HGSC	1	pT3c	fallopian tube	omentum	60%
3	T7116	72	IIIC	HGSC	1	pT3c	ovary	unknown	10%
4	T7135	43	unknown	LGSC	1	pT3	ovary	ovary	60%

Abbreviations: FIGO, International Federation of Gynecology and Obstetrics; LN, Lymph node metastasis(1, had lymph node metastasis; 0, had no lymph node metastasis); HGSC, High-Grade Serous Carcinoma; LGSC, Low-Grade Serous Carcinoma; T Nr., the numbers for tumor specimen; Tumor%, the amount of tumor contained in the specimen.

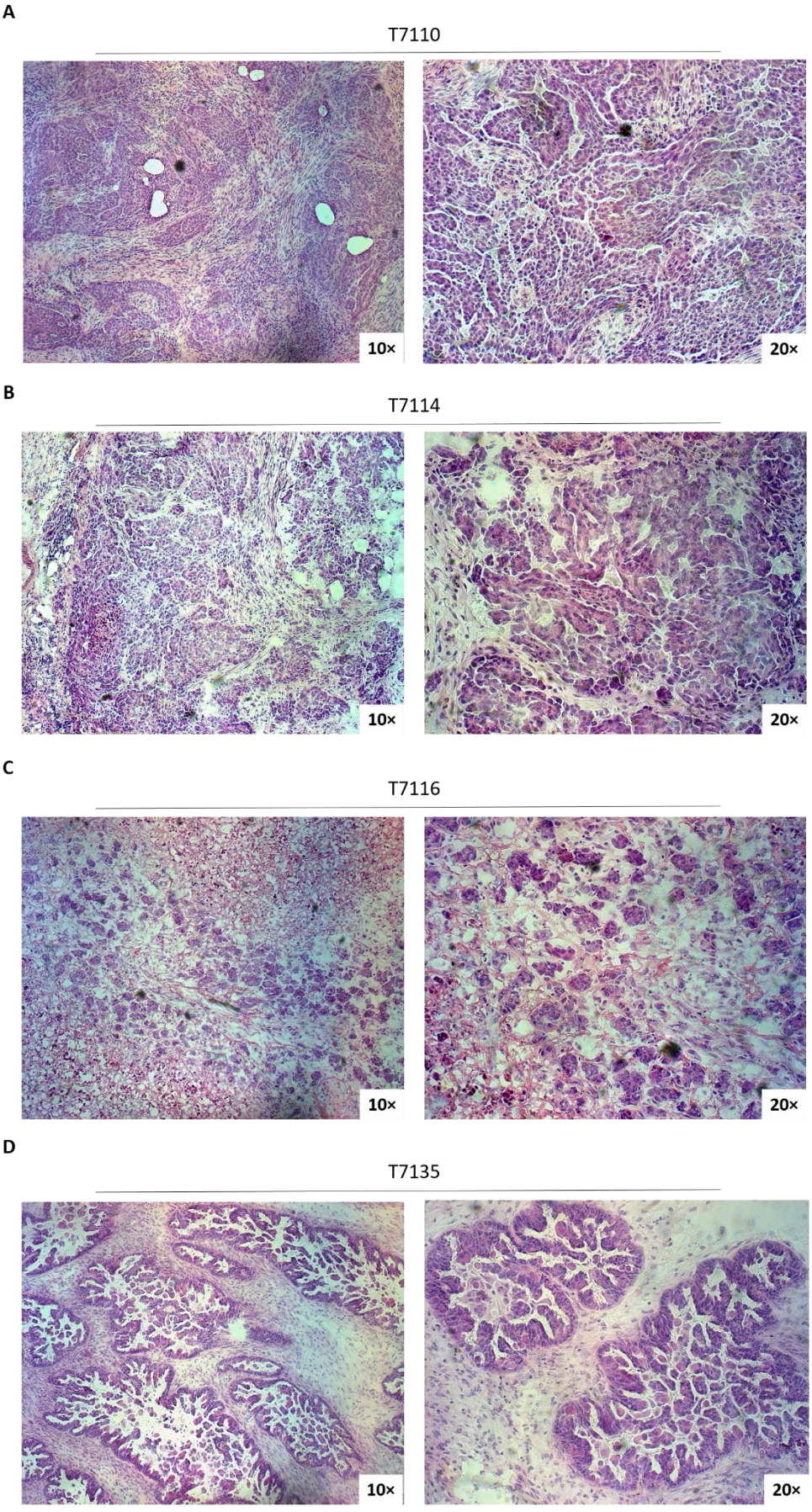

Figure 11 *Histopathology of 4 ovarian cancer samples by Hematoxylin and eosin staining (10x and 20x)*

A,B,C, 3 high-grade serous carcinomas from patient 1 to 3 individually, which presented severe nuclear atypia and high nuclear-to-cytoplasmic ratio;
D, low-grade serous carcinoma (LGSC) from patient4, which showed uniform nuclei and infrequent mitotic figures, with low nuclear atypia and a lower nuclear-to-cytoplasmic ratio; Magnifications are 10× and 20× for each tumor; T7110 (Tumor7110) from patient1, T7114 (Tumor7114) from patient2, T7116 (Tumor7116) from patient3, T7135 (Tumor7135) from patient4.

3.4.2 Adhesion molecules expressed in pairs of NADs and tumors

Proteins were isolated from 4 matched pairs of NADs and tumor tissue. 4 pairs are named as patient1, patient2, patient3, and patient4 in the following descriptions. The expression of E-Cadherin, Cytokeratin7, Vimentin, BCAM and ALCAM were measured by western blot. The results of western blot will be analyzed following three aspects as followed:

From the aspect of the origin of tumor tissue, expression of Cytokeratin 7 and E-Cadherin in patient4 tumor derived from ovary (primary tumor) were higher than in patient1, 2 and 3, where the tumor tissue was derived from omentum (metastasis) (patient3 specimen site is unknown) (Figure 12A, B).

From the aspect of NADs, NADs from HGSC (patient1, 2 and 3) expressed higher E-Cadherin, ALCAM and BCAM than NADs from LGSC (patient4). NADs from fallopian tumor (patient1, 2) had higher expression of BCAM than from ovarian tumor (patient3, 4), as well as lower expression of Cytokeratin 7 from fallopian tumor than from ovarian tumor (Figure 12A, B).

From the aspect of NAD-tumor tissue pairs, expression of E-Cadherin, Cytokeratin7, ALCAM and BCAM were clearly higher in NADs than in tumors from patient1 and patient3. However, for patient2 and patient4 it is hard to make a unified conclusion of expression patterns from this aspect. Cytokeratin 7 and E-Cadherin were expressed in all NADs and tumors pairs. Expression levels of Vimentin are higher in tumor tissue than in NADs in all pairs. ALCAM and BCAM expression present the similar pattern in patient1, 3 and 4, except patient2 (Figure 12A, B). Three cell lines: SKOV-3, OAW 42, and OVCAR-8 were loaded as positive controls. Each band was normalized to β-actin and positive control. Quantitative analysis were shown in Figure 12B.

A

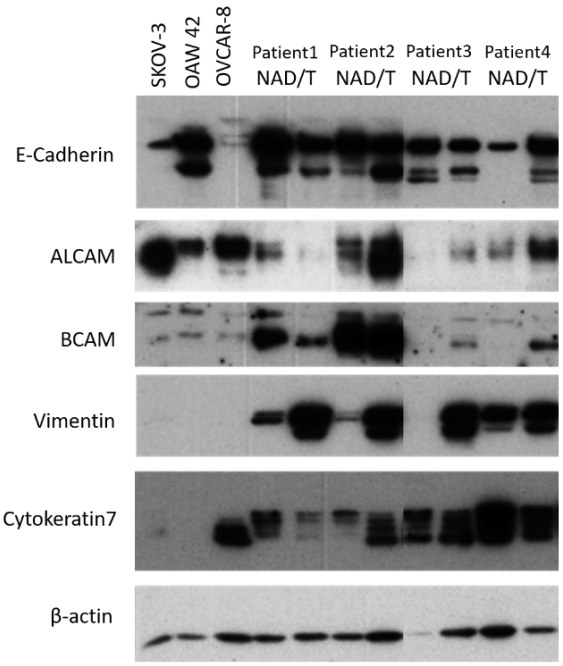

B

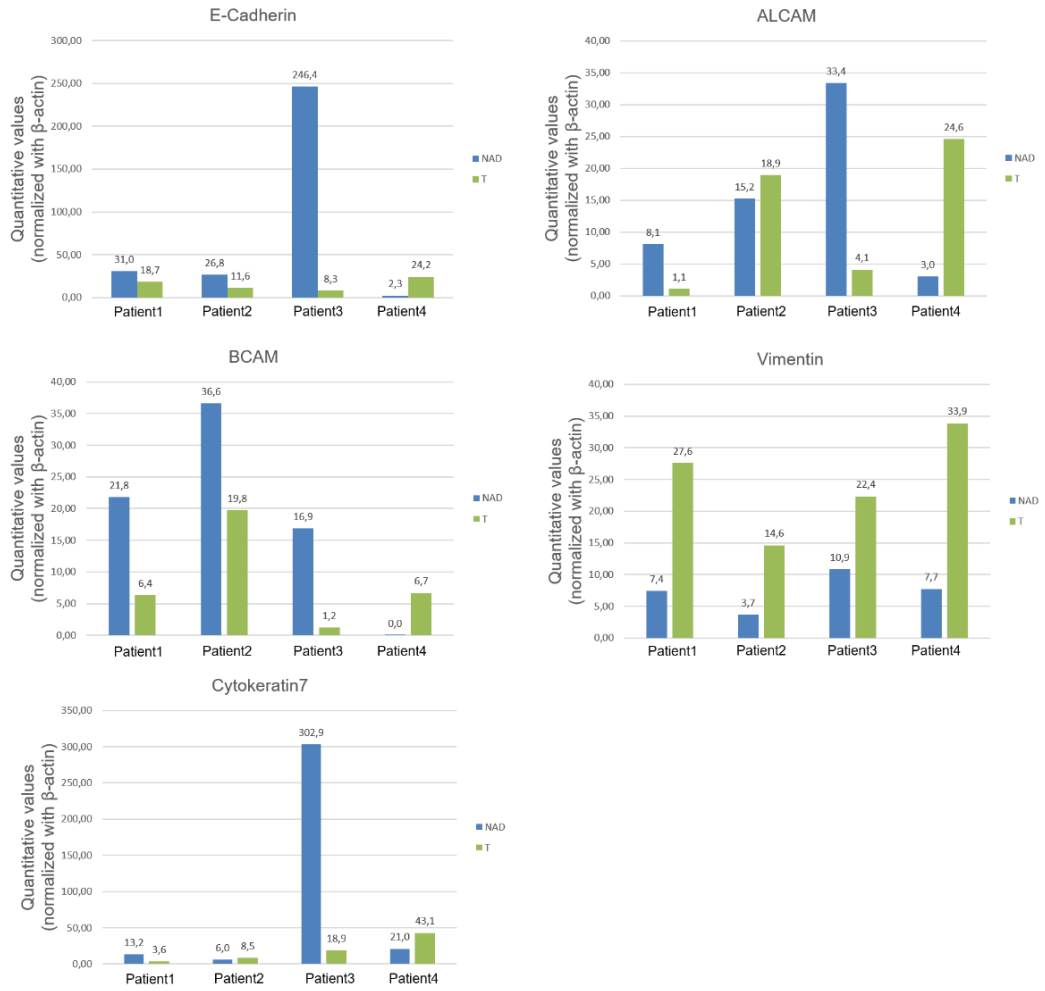

Figure 12 *Expression analysis of E-Cadherin, ALCAM, BCAM, Vimentin and Cytokertin7 level in NADs and Tumors*

A, western blot results from 4 pairs of NADs and Tumors. β-actin was used as endogenous control;

B, quantification of western blot results.

4 Discussion

Although hematogenous and lymphatic dissemination are the most common routes for metastasis, ovarian cancer frequently disseminate via transcoelomic route to develop peritoneal metastases[134, 135], which happened in up to 70% of ovarian advanced cancers[135]. Cancer cells detached from the primary tumor are transported as single cells or aggregates (spheroids) by peritoneal fluid to subsequently spread locally colonizing the peritoneum. Despite intensive research in the last decades, the key molecular players supporting spheroids aggregation and survival within the ascites and those involved in the subsequent cellular attachment to the peritoneal wall remain unknown. In this context, most of the published data are based on in vitro studies and/or used ovarian cancer cell lines[113, 136-138] rather than patient-derived cells. The aim of the actual work was to characterize different cell populations within the ascites fluid of ovarian cancer patients and further to analyze their behavior in vitro, especially regarding the expression of certain adhesion molecules.

In my doctoral thesis, I studied the properties of ADs (adherent cells) and NADs (non-adherent cells) cultured from ascites derived cells. NADs stand out from original ascites cell populations and contained mainly spheroids enriched with cells displaying epithelial and tumoral properties. In contrast, ADs, which grew after few a days as a monolayer also from the original ascites pellet were characterized by a mesenchymal phenotype and non-tumoral properties. Moreover, the use of cell strainer to purify the spheroids from the ascites-derived cells was essential for further analyses, which focused on the specific properties of tumor cells in ascites-derived cells. The analysis of the adhesion molecules expression pattern on the NADs and tumors, highlighted the importance of spheroids in the formation of OvCa metastasis.

4.1 Characteristics of ADs and NADs

ADs and NADs samples were stained with antibodies against established markers of immune cells (CD45), mesenchymal stem cells (CD90) and the tumor cells (EpCAM/CD24) and analyzed by FACS. ADs mainly consisted of CD90+ population, while most EpCAM+/CD24+ cells were found in NADs, which confirmed the tumoral properties of NADs, like previously described [139].

Adhesion molecules, e.g. E-cadherin, ALCAM, as well as other factors as cytokeratin 7 and vimentin were analyzed in cultured ascites-derived cells, ADs and NADs, by western blot. NADs, mostly consisting of spheroids, presented high epithelial characteristics compared to mesenchymal ADs, in line with a previous study[140]. Importantly, our study is the first one to analyze ALCAM, which might be involved in the formation of spheroids and further attachment to the metastatic site, but no apparent changes were observed when comparing ADs and NADs.

Here, we are aware of the limitations of this analysis: first, growth factors included in the ascites fluid, which are necessary for maintaining the properties of ADs and NADs are losing during culture time in normal medium for a long time. Therefore, the characteristics of ascites-derived cells are altered compared to the original state in peritoneal cavity. Also, ADs and NADs from different samples were cultured for different times ranging from 1-4 weeks, which may increase the difficulties to compare.

4.1.1 ADs

Ardian Latifiet al.[141] described the isolation of ovarian cancer cells from ascites by cultivating the ascites-derived cells in low attachment plates. The adherent growing population is what we call ADs can form after 2-3 days. Here, our study shows that, spindle-shaped ADs are mesenchymal-like with high proliferative capacity in vitro and high expression of one of the MSC markers, CD90. Regarding to the role of MSC in the peritoneal metastasis, one study[110] confirmed that the expression of CD90 in OvCa ascites-derived cells is much higher (0.04~6.81%, $p=0.001$) in patients with peritoneal metastasis compared to that without peritoneal metastasis (0.01~0.45%). Additionally, intraperitoneal co-injection of CD90+CD45- mesothelial-like cells with the human gastric cancer cell line, MKN45, significantly enhanced the rate of metastatic formation in the peritoneum of nude mice. Moreover, a study[142] using organotypic 3D cultures had found that primary human mesothelial cells with a mesenchymal phenotype secrete fibronectin in the presence of OvCa cells, and fibronectin are consistently overexpressed in the patients who have omental metastasis. Interestingly, another study[140] shows that intraperitoneal injection of only ascites-derived ADs did not lead to tumor growth and peritoneal metastasis in nude mice suggesting that mesothelial-like cells may merely play a tumor-supportive role during OvCa progression.

In our study, most ADs came from high grade OvCa which already form metastasis, and more frequently presented as fibroblast-like spindles. In this context, one study[143] confirmed that in peritoneal metastasis, a sizeable subpopulation of cancer-associated fibroblasts (CAFs) originates from mesothelial-like cells through a mesothelial-to-mesenchymal transition (MMT), which promotes adhesion, invasion, vascularization and subsequent tumor growth. However, it remains still unclear which cellular components are included in ADs and whether ADs are regulated by NADs.

4.1.2 NADs

4.1.2.1 Source of spheroids

A recent study [144] reported that spheroids predominantly arise from multicellular detachment from the primary tumor and are responsible for intraperitoneal metastasis. This results contradict the previous hypothesis of multicellular spheroids arising from single detached cells that aggregate within the abdomen [37] [145]. This recent results support a model in which spheroids are metastatic units, and that metastatic sites are formed from single spheroids that detached as groups of cells from the primary tumor[144].

4.1.2.2 Components of spheroids

Our analysis show that the spheroids from ascites contain EpCAM+/CD24+ tumor cells, CD45+ immune cells, and also some CD90+ mesothelial-like cells by FACS analysis. Recently, it had been confirmed that in the spheroids isolated from OvCa effusions, a core of mesothelial cells was encased in a shell of tumor cells, with partial expression of calretinin[137] or α-SMA[146] (markers of mesothelial cells). Mesothelial cells presented mesenchymal phenotype due to mesothelial to mesenchymal transition (MMT), which can explain why in our western blot and FACS analysis NADs expressed a little amount of vimentin and CD90.

Regarding to the immune cells in the ascites, our FACS analysis revealed a CD45+ subpopulation in the ascites spheroids, which is a broad marker for immune cells. In order to better characterize the different immune cells, specific markers such as CD3+ for lymphocytes T cells or CD163+ for macrophages must be used in the future. Recently, one study confirmed that CD45+ EpCAM+ populations in OvCa ascites were more drug resistant compared to EpCAM+ tumor cells due to the over-expression of

SIRT1, ABCA1 and BCL2 genes[147]. Moreover, in vivo data suggest that tumor-associated macrophages (TAMs) may promote spheroid formation and tumor growth. Here, TAMs were found within the spheroids, thereby secreting large amounts of epidermal growth factor (EGF), which leads to upregulation of integrin and ICAM-1 expression in tumor cells [10]. These findings above suggested the multicellular components of spheroids, and tumor cell to tumor cell/non-tumor cell contacts within the spheroids. Additionally, multicellular EOC (Epithelial Ovarian Cancer) spheroids are dynamic structures of proliferating, non-proliferating and hypoxic regions where homotypic and heterotypic cell interactions likely play a critical role[146]. Interestingly, single-cell RNA-seq techniques were used in a recent study[148] to investigate different cell populations within ovarian tumors. They found out that the proportion of these populations changes from primary to metastatic in a shift from mainly epithelial cells to leukocytes with few cancer epithelial cells in the metastases which suggested the importance of immune cells in the ovarian cancer progression.

4.1.2.3 Functions of spheroids

Furthermore, spheroids represent a more chemoresistant population since chemotherapeutic drugs show a lower incorporation and poor diffusion in such multicellular structures[149, 150]. Moreover, it has been suggested that chemoresistance is caused, in part, by tumor cells entering a non-cycling state with low metabolic activity, which is a characteristic feature of detached tumor cells and spheroids floating in the peritoneal fluid or ascites. Tumor cell interaction with other host cells has also been described to modulate chemoresistance[151, 152]. It should be noted that our study has examined the properties of the ascites-derived cells only in vitro, however a previous study[153] has showed that NAD epithelial spheroids which derived from chemotherapy resistance patients successfully established xenografted tumor, but ADs cannot.

4.2 Purify the tumor cells from ascites-derived cell populations

Epithelial cell adhesion molecule (EpCAM) and cluster of differentiation 24 (CD24) were confirmed as the highest sensitivity markers for OvCa ascites-derived tumor cells[154]. Since we have confirmed that spheroids are enriched of EpCAM+/CD24+ population, it become necessary and important to get rid of CD45 positive populations

and purify the spheroids for the following analysis including planed transcriptome analysis. In our study, we used two simple methods to separate the OvCa ascites-derived cells into two populations with different characteristics. One method is the filtration of cell pellet by cell strainers. Here, most EpCAM+/CD24+ and CD45- cell population were found in >10μm or >40μm fraction, while EpCAM-/CD24- and CD45+ cell population were mainly in the <10μm or <40μm fraction. Another method is to culture ascites-derived cells in low-attachment container with MCDB medium or clarified ascites for several days. Then, NADs, which are spheroids enriched, expressed high level of EpCAM or CD24, while ADs are mainly consist of CD90 positive cell populations. Both methods confirmed that, the spheroids-enriched cell population present high tumor properties which to some extent purify the spheroids from the original ascites-derived cells. Other methods such as EpCAM-coated[155] or magnetic separation columns[154] have also been used to isolate tumor cells or CD45 negative cells from ascites, but these methods are not only expensive but also time-consuming and not the optimal choice with limited amount of ascites pellet.

In our experience the most efficient way to enrich NADs from patient ascites is the filter method. However, due to the high range of cells types and sizes in ascites it is difficult to determine which cell strainer size is the best for fully purifying the spheroids and fully getting rid of the CD45+ and other non-tumor cells. Separation of NADs from ADs via cultivation on low attachment flasks is also efficient but may lead to a change in the cellular characteristics due to the different and artificial microenvironment *in vitro*. This may lead to false results when analyzing i.e. the transcriptome or proteasome of these cells.

4.3 Comparison of ascites-derived NADs and tumor tissue

Several studies already focused on the comparison of primary tumor and metastasis, however little work have been performed on the analysis of the differences between free-floating spheroids and solid tumor (primary or metastasis). Our study is based on the hypothesis that OvCa spheroids are essential for metastatic spread. Here, the understanding of how cell spheroids aggregate and survive and further attach to the mesothelial cells in the peritoneum is one main aspect of our research.

In an effort to find cell adhesion molecules differentially expressed in ascites cells versus the primary tumor we performed western blot analysis to study the expression pattern of several adhesion molecules such as E-Cadherin, ALCAM, and BCAM, also cytokeratin7 and Vimentin, in ascites-derived spheroids (NADs) and solid tumor (primary or metastasis). Although it's hard to get a conclusion due to the limited pairs of NADs and tumor from the same patients, this preliminary work successfully established a method to purify a tumor-rich cell population in tissue and ascites-derived cells. Importantly, ovarian cancer is known as a very heterogeneous entity, and metastatic lesions within the peritoneal cavity arise from different detached tumor cell spheroids and might represent/include different tumor subclones. Therefore, in future analysis when comparing tumor tissue versus spheroids it is important to include tumor tissue from different localizations that might comprise a higher clonality, which is rather representative of the disease. Also, transcriptome analysis will be performed on multicellular spheroids and tumor tissue from the same patient in order to identify those factors involved in the OvCa metastasis mediated by ascites-derived cells.

In conclusion, our study found that spheroids are present in many ascites from OvCa patients. Moreover, it has been confirmed that cultured NADs which are mainly composed of spheroids has higher expression of E-Cadherin, cytokeratin7, EpCAM, and CD24 compared to non-tumoral ADs, and can be successfully purified from the original cell populations using cell strainers. Since ascites-derived spheroids are considered "metastatic units" that attach to the peritoneum during disease progression, comparative analysis on the adhesive molecules of spheroids and corresponding tumor tissue from the same patients will give us more information about specific tumoral characteristics essential for OvCa metastasis.

5 Zusammenfassung

Aszites-abgeleitete Zellen von Eierstockkrebspatientinnen enthalten sowohl Sphäroide (Zellaggregate) als auch Einzelzellen. ADs (adhärente Zellen) und NADs (nicht adhärente Zellen) wurden gebildet und separiert, indem die vom Aszites abgeleiteten Zellen in Flaschen mit geringer Anhaftung entweder mit MCDB-Medium oder in Aszitesflüssigkeit kultiviert wurden. NADs, die hauptsächlich aus Sphäroiden bestehen, zeigten im Vergleich zu mesenchymalen ADs hohe epitheliale Eigenschaften. NADs weisen hohe Expressionslevel für EpCAM / CD24 auf, während ADs hauptsächlich CD90 exprimieren. Zellsiebe, die zur Anreicherung von Sphäroiden und zur Entfernung der meisten Einzelzellen verwendet wurden, erwiesen sich als gutes Werkzeug für die weitere Charakterisierung der vom Aszites abgeleiteten Sphäroide. Es wurden vorläufige Analysen zur Expression bestimmter Adhäsionsmoleküle (E-Cadherin und ALCAM) in Sphäroiden im Vergleich zu dem jeweiligen Tumorgewebe einer Patientin durchgeführt. Diese vergleichenden Analysen sollen weitere Informationen zu spezifischen Tumoreigenschaften aufzeigen, welche für die Eierstockkrebs-Metastasierung entscheidend sind.

Summary (English version)

Ascites-derived cells from ovarian cancer patients contain spheroids (cell aggregates) and single cells. ADs (adherent cells) and NADs (non-adherent cells) were formed separately when ascites-derived cells were cultured in low-attachment flasks with MCDB or ascites fluid. NADs, mostly consisting of spheroids, presented high epithelial characteristics compared to mesenchymal ADs. EpCAM/CD24 are intensively expressed in NADs, while ADs mainly expressed CD90. Cell strainers, which were used for enriching spheroids and getting rid of most single cells, were confirmed as a good tool for the following characterization on the ascites-derived spheroids. Preliminary analysis on the expression of certain adhesion molecules (E-Cadherin and ALCAM) in spheroids in comparison to matched tumor tissue from the same patients were performed. These comparative analysis will give us more information about specific tumoral characteristics essential for OvCa metastasis.

6 Abbreviations

AA/Bis-AA	Acrylamide/Bis-Acrylamide
ALCAM	Activated Leukocyte Cell Adhesion Molecule
APS	Ammonium Peroxydisulfate
BCA	Butyleyanoacrylate
BSA	Bovine Serum Albumin
CAM	Cell adhesion molecular
CD	Cluster of differentiation
DMSO	Dimethylsulfoxid
ECL	Enhanced chemiluminescence
EMT	Epithelial-mesenchymal transition
EpCAM	Epithelial cell adhesion molecule
EOC	Epithelial Ovarian Cancer
FACS	Fluorescence activated Cell Sorting
FCS	Fatal Calf Serum
FIGO	International Federation of Gynecology and Obstetrics
HKG	Housekeeping Gene
HE	Hematoxylin-eosin staining
MET	Mesenchymal-Epithelial Transition
OVCAR-8	Ovarian Carcinoma Cells-8
PBS	Dulbecco's Phosphate Buffered Saline
PVDF	Polyvinylidendiflourid
rpm	Rounds per minute
RT	Room temperature
SKOV-3	Sloan-Kettering ovarian 3
SDS	Sodium dodecyl sulfate polyacrylamide gel electrophoresis
TBS	Tris-buffered saline
TBST	Tris-buffered saline with Tween20
TEMED	N,N,N',N'-Tetramethylethylendiamin

7 References

1. Goff, B.A., et al., *Ovarian carcinoma diagnosis: results of a national ovarian cancer survey.* Cancer: Interdisciplinary International Journal of the American Cancer Society, 2000. **89**(10): p. 2068-2075.
2. Matulonis, U.A., et al., *Ovarian cancer.* Nat Rev Dis Primers, 2016. **2**: p. 16061.
3. Zhang, S., et al., *Frequencies of BRCA1 and BRCA2 mutations among 1,342 unselected patients with invasive ovarian cancer.* Gynecologic oncology, 2011. **121**(2): p. 353-357.
4. Alsop, K., S. Fereday, and C. Meldrum, *BRCA mutation frequency and patterns of treatment response in BRCA mutation–positive women with ovarian cancer: a report from the Australian Ovarian Cancer Study Group.* Journal of Clinical Oncology, 2012. **30**(21): p. 2654.
5. Moorman, P.G., et al., *Oral contraceptives and risk of ovarian cancer and breast cancer among high-risk women: a systematic review and meta-analysis.* 2013. **31**(33): p. 4188-4198.
6. Bassuk, S.S. and J.E.J.A.o.e. Manson, *Oral contraceptives and menopausal hormone therapy: relative and attributable risks of cardiovascular disease, cancer, and other health outcomes.* 2015. **25**(3): p. 193-200.
7. Friebel, T.M., S.M. Domchek, and T.R.J.J.o.t.N.C.I. Rebbeck, *Modifiers of cancer risk in BRCA1 and BRCA2 mutation carriers: a systematic review and meta-analysis.* 2014. **106**(6): p. dju091.
8. Rice, M.S., et al., *Tubal ligation, hysterectomy, unilateral oophorectomy, and risk of ovarian cancer in the Nurses' Health Studies.* 2014. **102**(1): p. 192-198. e3.
9. Gaitskell, K., et al., *Tubal ligation and ovarian cancer risk in a large cohort: Substantial variation by histological type.* 2016. **138**(5): p. 1076-1084.
10. Nagle, C., et al., *Obesity and survival among women with ovarian cancer: results from the Ovarian Cancer Association Consortium.* British journal of cancer, 2015. **113**(5): p. 817.
11. Cannioto, R.A. and K.B.J.G.o. Moysich, *Epithelial ovarian cancer and recreational physical activity: a review of the epidemiological literature and implications for exercise prescription.* 2015. **137**(3): p. 559-573.
12. Adam, R.A. and Y.G.J.J.o.t.A.C.o.S. Adam, *Malignant ascites: past, present, and future.* 2004. **198**(6): p. 999-1011.
13. Feldman, G.B., et al., *The role of lymphatic obstruction in the formation of ascites in a murine ovarian carcinoma.* 1972. **32**(8): p. 1663-1666.
14. Parsons, S.L., M.W. Lang, and R.J. Steele, *Malignant ascites: a 2-year review from a teaching hospital.* European Journal of Surgical Oncology, 1996. **22**(3): p. 237-239.
15. Szender, J.B., et al., *Impact of ascites volume on clinical outcomes in ovarian cancer: A cohort study.* 2017. **146**(3): p. 491-497.
16. Wels, J., et al., *Migratory neighbors and distant invaders: tumor-associated niche cells.* 2008. **22**(5): p. 559-574.
17. Bhowmick, N.A., E.G. Neilson, and H.L.J.N. Moses, *Stromal fibroblasts in cancer initiation and progression.* 2004. **432**(7015): p. 332.
18. Preston, C.C., et al., *Immunity and immune suppression in human ovarian cancer.* 2011. **3**(4): p. 539-556.

19. Reinartz, S., et al., *Mixed‐polarization phenotype of ascites‐associated macrophages in human ovarian carcinoma: correlation of CD163 expression, cytokine levels and early relapse.* 2014. **134**(1): p. 32-42.
20. Takaishi, K., et al., *Involvement of M2‐polarized macrophages in the ascites from advanced epithelial ovarian carcinoma in tumor progression via Stat3 activation.* 2010. **101**(10): p. 2128-2136.
21. Ahmed, N. and K.J.F.i.o. Stenvers, *Getting to know ovarian cancer ascites: opportunities for targeted therapy-based translational research.* 2013. **3**: p. 256.
22. Vaughan, S., et al., *Rethinking ovarian cancer: recommendations for improving outcomes.* 2011. **11**(10): p. 719.
23. Kipps, E., D.S. Tan, and S.B.J.N.R.C. Kaye, *Meeting the challenge of ascites in ovarian cancer: new avenues for therapy and research.* 2013. **13**(4): p. 273.
24. Worzfeld, T., et al., *The unique molecular and cellular microenvironment of ovarian cancer.* Frontiers in oncology, 2017. **7**: p. 24.
25. Ahmed, N. and K. Stenvers, *Getting to know ovarian cancer ascites: opportunities for targeted therapy-based translational research.* Frontiers in oncology, 2013. **3**: p. 256.
26. Kipps, E., D.S. Tan, and S.B. Kaye, *Meeting the challenge of ascites in ovarian cancer: new avenues for therapy and research.* Nature Reviews Cancer, 2013. **13**(4): p. 273.
27. Thibault, B., et al., *Ovarian cancer microenvironment: implications for cancer dissemination and chemoresistance acquisition.* Cancer and Metastasis Reviews, 2014. **33**(1): p. 17-39.
28. Condeelis, J. and J.W. Pollard, *Macrophages: obligate partners for tumor cell migration, invasion, and metastasis.* Cell, 2006. **124**(2): p. 263-266.
29. Hagemann, T., et al., *Regulation of macrophage function in tumors: the multifaceted role of NF-κB.* Blood, 2009. **113**(14): p. 3139-3146.
30. Lengyel, E., *Ovarian cancer development and metastasis.* The American journal of pathology, 2010. **177**(3): p. 1053-1064.
31. Kulbe, H., et al., *A dynamic inflammatory cytokine network in the human ovarian cancer microenvironment.* Cancer research, 2012. **72**(1): p. 66-75.
32. Rodriguez, G.C., et al., *Regulation of invasion of epithelial ovarian cancer by transforming growth factor-β.* Gynecologic oncology, 2001. **80**(2): p. 245-253.
33. Finkernagel, F., et al., *The transcriptional signature of human ovarian carcinoma macrophages is associated with extracellular matrix reorganization.* Oncotarget, 2016. **7**(46): p. 75339.
34. Duluc, D., et al., *Interferon‐γ reverses the immunosuppressive and protumoral properties and prevents the generation of human tumor‐associated macrophages.* International journal of cancer, 2009. **125**(2): p. 367-373.
35. Bellora, F., et al., *TLR activation of tumor‐associated macrophages from ovarian cancer patients triggers cytolytic activity of NK cells.* European journal of immunology, 2014. **44**(6): p. 1814-1822.
36. Reinartz, S., et al., *Mixed‐polarization phenotype of ascites‐associated macrophages in human ovarian carcinoma: correlation of CD163 expression, cytokine levels and early relapse.* International journal of cancer, 2014. **134**(1): p. 32-42.

37. Yin, M., et al., *Tumor-associated macrophages drive spheroid formation during early transcoelomic metastasis of ovarian cancer.* 2016. **126**(11): p. 4157-4173.
38. Zhang, L., et al., *Intratumoral T cells, recurrence, and survival in epithelial ovarian cancer.* 2003. **348**(3): p. 203-213.
39. Windbichler, G., et al., *Interferon-gamma in the first-line therapy of ovarian cancer: a randomized phase III trial.* British journal of cancer, 2000. **82**(6): p. 1138.
40. Marth, C., et al., *Interferon‐gamma in combination with carboplatin and paclitaxel as a safe and effective first‐line treatment option for advanced ovarian cancer: results of a phase I/II study.* International Journal of Gynecological Cancer, 2006. **16**(4): p. 1522-1528.
41. Lu, C., et al., *Gene alterations identified by expression profiling in tumor-associated endothelial cells from invasive ovarian carcinoma.* 2007. **67**(4): p. 1757-1768.
42. Musrap, N. and E.P.J.M.C.R. Diamandis, *Revisiting the complexity of the ovarian cancer microenvironment—clinical implications for treatment strategies.* 2012. **10**(10): p. 1254-1264.
43. Emese, Z., et al., *Immunotherapy for ovarian cancer: recent advances and perspectives.* Current Opinion in Oncology, 2014. **26**(5): p. 492-500.
44. Katia, S., et al., *TRANCE- and CD40 ligand-matured dendritic cells reveal MHC class I-restricted T cells specific for autologous tumor in late-stage ovarian cancer patients.* Clinical Cancer Research, 2003. **9**(4): p. 1517-1527.
45. Santin, A.D., et al., *In vitro induction of tumor-specific human lymphocyte antigen class I-restricted CD8 cytotoxic T lymphocytes by ovarian tumor antigen-pulsed autologous dendritic cells from patients with advanced ovarian cancer.* American Journal of Obstetrics & Gynecology, 2000. **183**(3): p. 601-609.
46. Hwang, W.-T., et al., *Prognostic significance of tumor-infiltrating T cells in ovarian cancer: a meta-analysis.* 2012. **124**(2): p. 192-198.
47. Yung, S. and T.M.J.B.R.I. Chan, *Pathophysiology of the peritoneal membrane during peritoneal dialysis: the role of hyaluronan.* 2011. **2011**.
48. Rynne-Vidal, A., et al., *The mesothelial origin of carcinoma associated-fibroblasts in peritoneal metastasis.* 2015. **7**(4): p. 1994-2011.
49. Matte, I., et al., *Role of malignant ascites on human mesothelial cells and their gene expression profiles.* 2014. **14**(1): p. 288.
50. Stadlmann, S., et al., *Ovarian carcinoma cells and IL-1β-activated human peritoneal mesothelial cells are possible sources of vascular endothelial growth factor in inflammatory and malignant peritoneal effusions.* 2005. **97**(3): p. 784-789.
51. Matte, I., P. Bessette, and A. Piché, *Ascites in ovarian cancer progression: opportunities for biomarker discovery and new avenues for targeted therapies*, in *Ascites-Physiopathology, Treatment, Complications and Prognosis*. 2017, IntechOpen.
52. Ilmer, M., et al., *Two sides of the same coin: stem cells in cancer and regenerative medicine.* 2014. **28**(7): p. 2748-2761.
53. Raja, F., N. Chopra, and J.J.a.o.O. Ledermann, *Optimal first-line treatment in ovarian cancer.* 2012. **23**(suppl_10): p. x118-x127.
54. Baer, P.C.J.W.j.o.s.c., *Adipose-derived mesenchymal stromal/stem cells: an update on their phenotype in vivo and in vitro.* 2014. **6**(3): p. 256.

55. Kang, B.-J., et al., *Differentiation of canine adipose tissue–derived mesenchymal stem cells towards endothelial progenitor cells.* 2014. **75**(7): p. 685-691.
56. Minteer, D.M., K.G. Marra, and J.P.J.C.i.p.s. Rubin, *Adipose stem cells: biology, safety, regulation, and regenerative potential.* 2015. **42**(2): p. 169-179.
57. Salem, H.K. and C.J.S.c. Thiemermann, *Mesenchymal stromal cells: current understanding and clinical status.* 2010. **28**(3): p. 585-596.
58. Zuk, P.A., et al., *Multilineage cells from human adipose tissue: implications for cell-based therapies.* 2001. **7**(2): p. 211-228.
59. Fathalla, M.J.O. and g. survey, *Factors in the causation and incidence of ovarian cancer.* 1972. **27**(11): p. 751-768.
60. Auersperg, N., et al. *The biology of ovarian cancer*. in *Seminars in oncology*. 1998.
61. Kindelberger, D.W., et al., *Intraepithelial carcinoma of the fimbria and pelvic serous carcinoma: evidence for a causal relationship.* 2007. **31**(2): p. 161-169.
62. Kurman, R.J. and I.-M.J.T.A.j.o.s.p. Shih, *The Origin and pathogenesis of epithelial ovarian cancer-a proposed unifying theory.* 2010. **34**(3): p. 433.
63. Medeiros, F., et al., *The tubal fimbria is a preferred site for early adenocarcinoma in women with familial ovarian cancer syndrome.* 2006. **30**(2): p. 230-236.
64. Perets, R., et al., *Transformation of the fallopian tube secretory epithelium leads to high-grade serous ovarian cancer in Brca; Tp53; Pten models.* 2013. **24**(6): p. 751-765.
65. Lee, Y., et al., *A candidate precursor to serous carcinoma that originates in the distal fallopian tube.* 2007. **211**(1): p. 26-35.
66. Crum, C.P., et al., *Through the glass darkly: intraepithelial neoplasia, top‐down differentiation, and the road to ovarian cancer.* 2013. **231**(4): p. 402-412.
67. Latifi, A., et al., *Isolation and characterization of tumor cells from the ascites of ovarian cancer patients: molecular phenotype of chemoresistant ovarian tumors.* 2012. **7**(10): p. e46858.
68. Desoize, B. and J.-C. Jardillier, *Multicellular resistance: a paradigm for clinical resistance?* Critical reviews in oncology/hematology, 2000. **36**(2-3): p. 193-207.
69. Ahmed, N., et al., *Ascites induces modulation of α6β1 integrin and urokinase plasminogen activator receptor expression and associated functions in ovarian carcinoma.* British Journal of Cancer, 2005. **92**(8): p. 1475.
70. Nuzhat, A., et al., *Integrin-linked kinase expression increases with ovarian tumour grade and is sustained by peritoneal tumour fluid.* Journal of Pathology, 2003. **201**(2): p. 229-37.
71. Mills, G.B., et al., *Ascitic fluid from human ovarian cancer patients contains growth factors necessary for intraperitoneal growth of human ovarian adenocarcinoma cells.* The Journal of clinical investigation, 1990. **86**(3): p. 851-855.
72. Mills, G.B., et al., *A putative new growth factor in ascitic fluid from ovarian cancer patients: identification, characterization, and mechanism of action.* Cancer research, 1988. **48**(5): p. 1066-1071.
73. Kryczek, I., et al., *IL-6 production in ovarian carcinoma is associated with histiotype and biological characteristics of the tumour and influences local immunity.* British journal of cancer, 2000. **82**(3): p. 621.

74. Penson, R.T., et al., *Cytokines IL‐1β, IL‐2, IL‐6, IL‐8, MCP‐1, GM‐CSF and TNFα in patients with epithelial ovarian cancer and their relationship to treatment with paclitaxel.* International journal of gynecological cancer, 2000. **10**(1): p. 33-41.
75. Obata, N.H., et al., *Effects of interleukin-6 on in vitro cell attachment, migration and invasion of human ovarian carcinoma.* Anticancer research, 1997. **17**(1A): p. 337-342.
76. Syed, V., et al., *Reproductive hormone-induced, STAT3-mediated interleukin 6 action in normal and malignant human ovarian surface epithelial cells.* Journal of the National Cancer Institute, 2002. **94**(8): p. 617-629.
77. Wang, Y., et al., *Autocrine production of interleukin-6 confers cisplatin and paclitaxel resistance in ovarian cancer cells.* Cancer letters, 2010. **295**(1): p. 110-123.
78. Cohen, S., et al., *Platinum-resistance in ovarian cancer cells is mediated by IL-6 secretion via the increased expression of its target cIAP-2.* Journal of Molecular Medicine, 2013. **91**(3): p. 357-368.
79. Huang, S., et al., *Blockade of nuclear factor-κB signaling inhibits angiogenesis and tumorigenicity of human ovarian cancer cells by suppressing expression of vascular endothelial growth factor and interleukin 8.* Cancer research, 2000. **60**(19): p. 5334-5339.
80. Yoneda, J., et al., *Expression of angiogenesis-related genes and progression of human ovarian carcinomas in nude mice.* JNCI: Journal of the National Cancer Institute, 1998. **90**(6): p. 447-454.
81. Lane, D., et al., *Prognostic significance of IL-6 and IL-8 ascites levels in ovarian cancer patients.* BMC cancer, 2011. **11**(1): p. 210.
82. Hagemann, T., et al., *Ovarian cancer cells polarize macrophages toward a tumor-associated phenotype.* The Journal of Immunology, 2006. **176**(8): p. 5023-5032.
83. Balkwill, F., *Cancer and the chemokine network.* Nature Reviews Cancer, 2004. **4**(7): p. 540.
84. Wang, E., et al., *Peritoneal and subperitoneal stroma may facilitate regional spread of ovarian cancer.* Clinical cancer research, 2005. **11**(1): p. 113-122.
85. Belotti, D., et al., *Matrix metalloproteinases (MMP9 and MMP2) induce the release of vascular endothelial growth factor (VEGF) by ovarian carcinoma cells: implications for ascites formation.* Cancer research, 2003. **63**(17): p. 5224-5229.
86. Lin, Y.G., et al., *EphA2 overexpression is associated with angiogenesis in ovarian cancer.* Cancer, 2007. **109**(2): p. 332-340.
87. Yang, X., et al., *New ways to successfully target tumor vasculature in ovarian cancer.* Current opinion in obstetrics & gynecology, 2015. **27**(1): p. 58.
88. Yamamoto, S., et al., *Expression of vascular endothelial growth factor (VEGF) in epithelial ovarian neoplasms: correlation with clinicopathology and patient survival, and analysis of serum VEGF levels.* British journal of cancer, 1997. **76**(9): p. 1221.
89. Hartenbach, E., et al., *Vascular endothelial growth factor (VEGF) expression and survival in human epithelial ovarian carcinomas.* Cancer letters, 1997. **121**(2): p. 169-175.
90. Kassim, S.K., et al., *Vascular endothelial growth factor and interleukin-8 are associated with poor prognosis in epithelial ovarian cancer patients.* Clinical biochemistry, 2004. **37**(5): p. 363-369.

91. Bottsford-Miller, J.N., R.L. Coleman, and A.K. Sood, *Resistance and escape from antiangiogenesis therapy: clinical implications and future strategies.* Journal of Clinical Oncology, 2012. **30**(32): p. 4026.
92. Lu, C., et al., *Gene alterations identified by expression profiling in tumor-associated endothelial cells from invasive ovarian carcinoma.* Cancer research, 2007. **67**(4): p. 1757-1768.
93. Jee Young, H., et al., *Clinical and biological significance of tissue transglutaminase in ovarian carcinoma.* 2008. **68**(14): p. 5849-5858.
94. Minati, S., et al., *Enhanced peritoneal ovarian tumor dissemination by tissue transglutaminase.* 2007. **67**(15): p. 7194-7202.
95. Okegawa, T., et al., *The role of cell adhesion molecule in cancer progression and its application in cancer therapy.* Acta Biochimica Polonica-English Edition-, 2004. **51**: p. 445-458.
96. Al Habyan, S., et al., *Multicellular detachment generates metastatic spheroids during intra-abdominal dissemination in epithelial ovarian cancer.* 2018. **37**(37): p. 5127.
97. Lengyel, E.J.T.A.j.o.p., *Ovarian cancer development and metastasis.* 2010. **177**(3): p. 1053-1064.
98. Davidson, B., et al., *Expression of membrane-type 1, 2, and 3 matrix metalloproteinases messenger RNA in ovarian carcinoma cells in serous effusions.* 2001. **115**(4): p. 517-524.
99. Ernst, L.J.A.J.o.P., *Ovarian cancer development and metastasis.* 2010. **177**(3): p. 1053-1064.
100. Symowicz, J., et al., *Engagement of collagen-binding integrins promotes matrix metalloproteinase-9–dependent E-cadherin ectodomain shedding in ovarian carcinoma cells.* 2007. **67**(5): p. 2030-2039.
101. Moss, N.M., et al., *Ovarian cancer cell detachment and multicellular aggregate formation are regulated by membrane type 1 matrix metalloproteinase: a potential role in Ip metastatic dissemination.* 2009. **69**(17): p. 7121-7129.
102. Kenny, H.A., et al., *Mesothelial cells promote early ovarian cancer metastasis through fibronectin secretion.* The Journal of clinical investigation, 2014. **124**(10): p. 4614-4628.
103. Slack-Davis, J.K., et al., *Vascular Cell Adhesion Molecule-1 Is a Regulator of Ovarian Cancer Peritoneal Metastasis.* 2009. **69**(4): p. 1469-1476.
104. Frankel, A., ., R. Buckman, ., and R.S. Kerbel, %J Cancer Research, *Abrogation of taxol-induced G2-M arrest and apoptosis in human ovarian cancer cells grown as multicellular tumor spheroids.* 1997. **57**(12): p. 2388-93.
105. Shield, K., et al., *α2β1 integrin affects metastatic potential of ovarian carcinoma spheroids by supporting disaggregation and proteolysis.* 2007. **6**: p. 11.
106. Davidson, B., et al., *αV-and β1-integrin subunits are commonly expressed in malignant effusions from ovarian carcinoma patients.* 2003. **90**(2): p. 248-257.
107. Green, S.K., et al., *Antiadhesive antibodies targeting E-cadherin sensitize multicellular tumor spheroids to chemotherapy in vitro.* 2004. **3**(2): p. 149-159.
108. Daya, D., . and W.T. Mccaughey, %J Seminars in Diagnostic Pathology, *Pathology of the peritoneum: a review of selected topics.* 1991. **8**(4): p. 277-89.
109. Kenny, H.A., et al., *Use of a novel 3D culture model to elucidate the role of mesothelial cells, fibroblasts and extra-cellular matrices on adhesion and invasion of ovarian cancer cells to the omentum.* 2010. **121**(7): p. 1463-1472.

110. Kitayama, J., et al., *CD90 (+) mesothelial-like cells in peritoneal fluid promote peritoneal metastasis by forming a tumor permissive microenvironment.* 2014. **9**(1): p. e86516.
111. Kenny, H.A., et al., *Use of a novel 3D culture model to elucidate the role of mesothelial cells, fibroblasts and extra‐cellular matrices on adhesion and invasion of ovarian cancer cells to the omentum.* 2007. **121**(7): p. 1463-1472.
112. Witz, C.A., et al., *Composition of the extracellular matrix of the peritoneum.* 2001. **8**(5): p. 299-304.
113. Kenny, H., S. Dogan, and M.J.C.T.R. Zillhardt, *K Mitra A, Yamada SD, Krausz T, et al. Organotypic models of metastasis: a three-dimensional culture mimicking the human peritoneum and omentum for the study of the early steps of ovarian cancer metastasis.* 2009. **149**: p. 335-51.
114. Kenny, H.A., et al., *The initial steps of ovarian cancer cell metastasis are mediated by MMP-2 cleavage of vitronectin and fibronectin.* 2008. **118**(4): p. 1367-1379.
115. Iwanicki, M.P., et al., *Ovarian cancer spheroids use myosin-generated force to clear the mesothelium.* 2011. **1**(2): p. 144-157.
116. LIAW, Y.-S., et al., *Expression of integrins in human cultured mesothelial cells: the roles in cell-to-extracellular matrix adhesion and inhibition by RGD-containing peptide.* 2001. **95**(3): p. 221-226.
117. Burleson, K.M., et al., *Ovarian carcinoma ascites spheroids adhere to extracellular matrix components and mesothelial cell monolayers.* 2004. **93**(1): p. 170-181.
118. Lessan, K., et al., *CD44 and β1 integrin mediate ovarian carcinoma cell adhesion to peritoneal mesothelial cells.* 1999. **154**(5): p. 1525-1537.
119. Strobel, T. and S.A.J.G.o. Cannistra, *β1-integrins partly mediate binding of ovarian cancer cells to peritoneal mesothelium in vitro.* 1999. **73**(3): p. 362-367.
120. Strobel, T. and S.A.J.G.O. Cannistra, *Beta1-integrins partly mediate binding of ovarian cancer cells to peritoneal mesothelium in vitro.* 1999. **73**(3): p. 362-367.
121. Sawada, K., et al., *c-Met overexpression is a prognostic factor in ovarian cancer and an effective target for inhibition of peritoneal dissemination and invasion.* 2007. **67**(4): p. 1670-1679.
122. Nakamura, K., et al., *Exosomes promote ovarian cancer cell invasion through transfer of CD44 to peritoneal mesothelial cells.* 2017. **15**(1): p. 78-92.
123. Ahmed, N., et al., *Role of integrin receptors for fibronectin, collagen and laminin in the regulation of ovarian carcinoma functions in response to a matrix microenvironment.* 2005. **22**(5): p. 391-402.
124. Hunter, K.W., N.P. Crawford, and J.J.B.C.R. Alsarraj, *Mechanisms of metastasis.* 2004. **22**(3): p. 209-216.
125. Coleman, R.E. and S.A.J.C. Eccles, *General mechanisms of metastasis.* 1997. **80**(8 Suppl): p. 1529.
126. Kim, I., ., et al., *Vascular endothelial growth factor expression of intercellular adhesion molecule 1 (ICAM-1), vascular cell adhesion molecule 1 (VCAM-1), and E-selectin through nuclear factor-kappa B activation in endothelial cells.* 2001. **276**(10): p. 7614-20.
127. Enciso, J.M., et al., *Elevated glucose inhibits VEGF-A-mediated endocardial cushion formation: modulation by PECAM-1 and MMP-2.* 2003. **160**(4): p. 605-615.

128. Mohanraj, R., K. Antonina, and C.J.C.R. Subroto, *Novel role of lactosylceramide in vascular endothelial growth factor-mediated angiogenesis in human endothelial cells.* 2005. **97**(8): p. 796.
129. Deng, C., et al., *Angiogenic Effect of Intercellular Adhesion Molecule-1.* 2007. **27**(1): p. 9-12.
130. Kevil, C.G., et al., *Intercellular adhesion molecule-1 (ICAM-1) regulates endothelial cell motility through a nitric oxide-dependent pathway.* 2004. **279**(18): p. 19230-8.
131. Ding, Y.B., et al., *Association of VCAM-1 overexpression with oncogenesis,tumor angiogenesis and metastasis of gastric carcinoma.* 2003. **9**(7): p. 1409-1414.
132. Dita, G., et al., *Platelet-endothelial cell adhesion molecule-1 modulates endothelial migration through its immunoreceptor tyrosine-based inhibitory motif.* 2003. **301**(1): p. 243-249.
133. Sunyoung, P., et al., *PECAM-1 regulates proangiogenic properties of endothelial cells through modulation of cell-cell and cell-matrix interactions.* 2010. **299**(6): p. 1468-84.
134. De Cuba, E., et al., *Understanding molecular mechanisms in peritoneal dissemination of colorectal cancer.* 2012. **461**(3): p. 231-243.
135. Tan, D.S., R. Agarwal, and S.B.J.T.l.o. Kaye, *Mechanisms of transcoelomic metastasis in ovarian cancer.* 2006. **7**(11): p. 925-934.
136. Hebron, K.E., et al., *Alternative splicing of ALCAM enables tunable regulation of cell-cell adhesion through differential proteolysis.* 2018. **8**(1): p. 3208.
137. Shishido, A., et al., *Mesothelial cells facilitate cancer stem□like properties in spheroids of ovarian cancer cells.* 2018. **40**(4): p. 2105-2114.
138. Rosso, M., et al., *E-cadherin: A determinant molecule associated with ovarian cancer progression, dissemination and aggressiveness.* 2017. **12**(9): p. e0184439.
139. !!! INVALID CITATION !!! [140].
140. Latifi, A., et al., *Isolation and characterization of tumor cells from the ascites of ovarian cancer patients: molecular phenotype of chemoresistant ovarian tumors.* PLoS One, 2012. **7**(10): p. e46858.
141. Shepherd, T.G., et al., *Primary culture of ovarian surface epithelial cells and ascites-derived ovarian cancer cells from patients.* 2006. **1**(6): p. 2643.
142. Kenny, H.A., et al., *Mesothelial cells promote early ovarian cancer metastasis through fibronectin secretion.* 2014. **124**(10): p. 4614-4628.
143. Sandoval, P., et al., *Carcinoma‐associated fibroblasts derive from mesothelial cells via mesothelial‐to‐mesenchymal transition in peritoneal metastasis.* 2013. **231**(4): p. 517-531.
144. Al Habyan, S., et al., *Multicellular detachment generates metastatic spheroids during intra-abdominal dissemination in epithelial ovarian cancer.* 2018: p. 1.
145. Shield, K., et al., *Multicellular spheroids in ovarian cancer metastases: Biology and pathology.* 2009. **113**(1): p. 143-148.
146. Matte, I., et al., *Mesothelial cells interact with tumor cells for the formation of ovarian cancer multicellular spheroids in peritoneal effusions.* 2016. **33**(8): p. 839-852.
147. Akhter, M.Z., et al., *Aggressive serous epithelial ovarian cancer is potentially propagated by EpCAM+ CD45+ phenotype.* 2018. **37**(16): p. 2089.

148. Shih, A.J., et al., *Identification of grade and origin specific cell populations in serous epithelial ovarian cancer by single cell RNA-seq.* 2018. **13**(11): p. e0206785.
149. Fayad, W., et al., *Restriction of cisplatin induction of acute apoptosis to a subpopulation of cells in a three‐dimensional carcinoma culture model.* 2009. **125**(10): p. 2450-2455.
150. Tannock, I.F., et al., *Limited penetration of anticancer drugs through tumor tissue: a potential cause of resistance of solid tumors to chemotherapy.* 2002. **8**(3): p. 878-884.
151. Yeung, C.L.A., et al., *Exosomal transfer of stroma-derived miR21 confers paclitaxel resistance in ovarian cancer cells through targeting APAF1.* 2016. **7**: p. 11150.
152. Wang, W., et al., *Effector T cells abrogate stroma-mediated chemoresistance in ovarian cancer.* 2016. **165**(5): p. 1092-1105.
153. Latifi, A., et al., *Isolation and characterization of tumor cells from the ascites of ovarian cancer patients: molecular phenotype of chemoresistant ovarian tumors.* PloS one, 2012. **7**(10): p. e46858.
154. Peterson, V.M., et al., *Ascites analysis by a microfluidic chip allows tumor-cell profiling.* 2013. **110**(51): p. E4978-E4986.
155. Antolovic, D., et al., *Heterogeneous detection of circulating tumor cells in patients with colorectal cancer by immunomagnetic enrichment using different EpCAM-specific antibodies.* 2010. **10**(1): p. 35.

8 Acknowledgments

Many thanks to my supervisor PD. Dr. Leticia Oliveira-Ferrer, who offered me this opportunity to join this promising project and always guide the project to a right direction. Many thanks to Prof. Schmalfeldt, who supports my project and offer us continuous samples from clinic. Many thanks to the patients involved in this project who gave us precious material for the scientific research.

I am grateful to Dr. Karen Legler (post-doc) and Ms. Fabienne Hamester (PhD student) who have a broad expertise on molecular biology and biochemistry techniques, gave me useful advices when I have difficulties during my experiments. I am also grateful to Ms. Kathrin Eylmann and Ms. Maila Rossberg, who assist with the HE staining and the cell culture. Many thanks to Vera Labitzky from Institute of Anatomy and Experimental Morphology, who gave lots of support to this project.

Many thanks to UKE FACs core facility who offer us opportunities to do the analysis there and technique supports.

Thanks to Chinese Scholarship Council (CSC) founding my study in Germany.
Last but not least, I am also very grateful to my husband, my parents and all my friends in China who gave me lots of encourages and supports during my work in Germany.

9 Curriculum vitae

The CV has been removed for data protection reasons.

10 Declaration of an oath

Ich versichere ausdrücklich, dass ich die Arbeit selbständig und ohne fremde Hilfe verfasst, andere als die von mir angegebenen Quellen und Hilfsmittel nicht benutzt und die aus den benutzten Werken wörtlich oder inhaltlich entnommenen Stellen einzeln nach Ausgabe (Auflage und Jahr des Erscheinens), Band und Seite des benutzten Werkes kenntlich gemacht habe.
Ferner versichere ich, dass ich die Dissertation bisher nicht einem Fachvertreter an einer anderen Hochschule zur Überprüfung vorgelegt oder mich anderweitig um Zulassung zur Promotion beworben habe.
Ich erkläre mich einverstanden, dass meine Dissertation vom Dekanat der Medizinischen Fakultät mit einer gängigen Software zur Erkennung von Plagiaten überprüft werden kann.

Unterschrift:  .....